Aus dem Institut für Biochemie und Molekularbiologie II

Direktor: Univ.-Prof. Dr. J. Scheller

Dominant-negative overexpression models of proliferative functions of human B23 and C23

Dissertation

zur Erlangung des Grades eines Doktors der Medizin

der Medizinischen Fakultät der Heinrich-Heine-Universität Düsseldorf

vorgelegt von

Timo Jendrik Faustmann

2018

Als Inauguraldissertation gedruckt mit Genehmigung der Medizinischen

Fakultät der Heinrich-Heine-Universität Düsseldorf

gez.: Timo Jendrik Faustmann

Dekan: Prof. Dr. Nikolaj Klöcker

Erstgutachter: Prof. Dr. Reza Ahmadian

Zweitgutachter: Prof. Dr. Nikolas Stoecklein

Dedicated to Anna and my family.

Abstract

Background: The multifunctional, nucleolar proteins nucleophosmin (B23) and nucleolin (C23) are involved in different cellular processes in normal and transformed cells. Both proteins are highly expressed in dividing cells and are regulators of gene expression, rRNA synthesis, and protein and RNA transport during cell proliferation. The multitude of functions of nucleolin and nucleophosmin are reflected by their multidomain architecture. However, the functional relationship between the subdomains of nucleophosmin and nucleolin, their subcellular localization and their function in proliferative and survival signalling remains unclear so far.

Aim: This study aims at identifying nucleophosmin and nucleolin subdomains with dominant- negative effects on tumour cell proliferation.

Methods: The methods and techniques used were cloning, eukaryotic overexpression of defined nucleophosmin and nucleolin subdomains in cell culture (HeLa and Cos-7 cell lines) along with comparative analysis of proliferation and viability (MTT assay, FACS-based analysis of DNA amount) as well as subcellular localization by confocal microscopy.

Results: Following the transient overexpression of the C-terminal RNA-binding and glycine-arginine-rich domains (RRM4GAR) of nucleolin, MTT assays revealed a reduction of 40 % for HeLa cells and 20 % for Cos-7 cells in proliferation, respectively. The reduction observed was significant on a $p < 0.001$ level in HeLa cells and significant on a $p < 0.01$ level in Cos-7 cells. In agreement, herewith, both cell lines showed increased SubG1 fractions in FACS analysis. Further antiproliferative activities could be ascribed to the glycine-arginine-rich (GAR) domain of nucleolin and the histone-RNA-binding domain (HBD-RNABD) of nucleophosmin. The RRM4GAR and GAR domains were found localized in the cytoplasm and the HBD-RNABD in the nucleus using confocal imaging.

Conclusion: The dominant-negative effects of the RRM4GAR, GAR and HBD-RNABD demonstrated in HeLa and Cos-7 cells point out the importance of the C-terminus of nucleophosmin and nucleolin in the proliferation of primate and human tumour cell lines. These findings provide a lead for further investigations concerning the structure and function of these nucleolar proteins. The subdomains identified are possible targets for an antiproliferative tumour therapy.

Zusammenfassung

Hintergrund: Die multifunktionalen, primär nukleolären Proteine Nucleophosmin (B23) und Nucleolin (C23) sind wichtige, direkt mit der Tumorentstehung assoziierte Proteine. Sie werden in hohem Maß in proliferativen Zellen exprimiert und sind in der Regulation von Genexpression, rRNA-Synthese sowie Protein- und RNA-Transport während der Proliferation involviert. Der funktionelle Zusammenhang zwischen der Domänenstruktur von Nucleophosmin und Nucleolin, der subzellulären Lokalisation und der Funktion in Proliferation und *survival* ist größtenteils unverstanden.

Ziel: Das Ziel dieser Arbeit war die Identifikation von Nucleophosmin- und Nucleolin-Domänen mit dominant-negativer Wirkung auf die Tumorzellproliferation.

Methodik: Die verwendeten Methoden und Technologien waren Klonierung und eukaryotische Überexpression definierter Domänen von Nucleophosmin und Nucleolin in Zellkultur (HeLa-, Cos-7-Zellen) mit vergleichender Analyse von Proliferation und Viabilität (MTT assay, FACS-basierte DNA-Gehaltsanalyse) sowie subzellulärer Lokalisation mittels Konfokal-Mikroskopie.

Ergebnisse: HeLa-Zellen zeigen im MTT-Assay nach transienter Überexpression der C-terminalen RNA-bindenden und Glycin-Arginin-reichen Domänen (RRM4GAR) von Nucleolin, eine um 40% signifikant ($p<0.001$) und Cos-7-Zellen eine um 20% signifikant ($p<0.01$) verminderte Proliferation im Vergleich zur „Leer-Vektor-Kontrolle“. Übereinstimmend hiermit sind in der FACS-Analyse die SubG1-Fraktionen in beiden Zelllinien signifikant erhöht. Weitere antiproliferativ-wirkende Domänen sind die Histon-RNA-bindende-Domäne (HBD-RNABD) von Nucleophosmin und die Glycin-Arginin-reiche Domäne (GAR) von Nucleolin. Konfokal-mikroskopisch sind die RRM4GAR- und GAR-Domäne im Zytoplasma und die HBD-RNABD im Nukleus lokalisiert.

Schlussfolgerung: Die hier nachgewiesenen dominant-negativen Effekte in HeLa- und Cos7-Zellen unterstreichen die Bedeutung der C-Termini von Nucleophosmin und Nucleolin in der Proliferation humaner Tumorzellen. Die erwähnten Domänen ermöglichen weitere gezielte Untersuchungen zur Struktur-Funktionsanalyse nukleolärer Proteine und sind mögliche Zielstrukturen für eine antiproliferative Tumortherapie.

List of Abbreviations

293T cells	human embryonic kidney cells
α-tubulin	alfa-tubulin
aa	amino acid
ADP	adenosine diphosphate
AMC	7-Amino-4-methylcumarin
AML	acute myeloid leukaemia
ANOVA	analysis of variance
APS	ammonium persulphate
ARF	adenosine diphosphate ribosylation factor
B23	nucleophosmin
Bam HI	restriction enzyme *Bam HI*
Bcl2	B-cell lymphoma 2 protein
bp	base pair
BSA	bovine serum albumin
C23	nucleolin
Ca^{2+}	calcium
CAT	chloramphenicol acetyltransferase
CD34	cluster of differentiation 34
cdc2	cyclin-dependent kinase 2
CHAPS	3-((3-cholamidopropyl) dimethylammonio)-1-propanesulphonate
CK2	casein kinase 2
CLSM	Confocal laser scanning microscopy
c-Myc	cellular-myelocytomatose-oncogene
CO_2	carbon dioxide
Cos-7	monkey-derived kidney cells
C-terminus	Carboxy Terminus
DAPI	4′,6-diamidin-2-phenylindol
ddH_2O	double-distilled water
DEVD	amino acid sequence Aspartic Acid-Glutamic Acid-Valine-Aspartic Acid
$DMEM^{+/+}$	Dulbecco's Modified Eagle Medium with 10 % foetal calf serum and 1 % penicillin and streptomycin
$DMEM^{-/-}$	Dulbecco's Modified Eagle Medium without 10 % foetal calf serum and 1 % penicillin and streptomycin
DMSO	dimethyl sulphoxide
DNA	deoxyribonucleic acid
dNTP	desoxyribonucleotide triphosphate
DT40	chicken-derived B-cell line
DTT	dithiothreitol
E. coli	*Escherichia coli*
ECL	electrogenerated chemiluminescence
ECM	evolutionary conserved motif
EDTA	Dinatrium-Ethylendiamin - tetraacetate

FACS	fluorescence activated cell sorting
FastAP	thermosensitive alkaline phosphatase
FMRP	fragile mental retardation protein
G0 phase	gap 0 phase
G1 phase	gap 1 phase
G2 phase	gap 2 phase
GAR	glycine-arginine-rich domain of nucleolin
GFP	green fluorescent protein
H1	histone 1
H3	histone 3
HBD	histone-binding domain
HCL	hydrochloride
Hdm2	human double minute 2 protein
HEK293	human embryonic kidney cells
HeLa	human cervix carcinoma cells
HepG2	hepatocellular carcinoma cells
HEPES	(4-(2-hydroxyethyl)-1-piperazineethanesulphonic acid)
HIV	human immunodeficiency virus
HL-60	human promyelocytic leukaemia cells
HSV-1	herpes simplex virus type 1
hTERT	human telomerase reverse transcriptase subunit
Huh7	hepatocellular carcinoma cells
IDR	intrinsically disordered regions
K562	human erythromyeloblastoid leukaemia cell line
Kb	kilobase
KCL	potassium chloride
kDa	kilodalton
L929	mouse fibroblast cells
LB media	lysogeny broth media
MEFs	mouse embryo fibroblasts
Mdm2	mouse double minute 2 protein
Mg^{2+}	magnesium
$MgCl_2$	magnesium chloride
M phase	mitosis phase
mRNA	messenger ribonucleic acid
MSCs	mesenchymal stem cells
MTT	3-(4,5-dimethylthiazol-2-yl)-2,5-diphenyl tetrazolium bromide
MW	molecular weight
Myc	myelocytomatose oncogene
NaCl	sodium chloride
Na-Citrate	sodium citrate
NADPH	nicotinamide adenine dinucleotide phosphate
NADH	nicotinamide adenine dinucleotide
NaOH	sodium hydroxide
Ncl	nucleolin
Nclfl	full-length nucleolin
NclN-Term	N-terminus of nucleolin
NclN-TermRRM1	N-terminus and RNA recognition motif 1 of nucleolin
NclRRM14GAR	C-terminus of nucleolin

NclRRM12	RNA recognition motif 1 and 2 of nucleolin
NclRRM34	RNA recognition motif 3 and 4 of nucleolin
NclRRM4GAR	RNA recognition motif 4 together with the glycine-arginine-rich domain of nucleolin
NclGAR	glycinie-arginine-rich domain of nucleolin
NES	nuclear export signal
NLS	nuclear localization signal
Not I	restriction enzyme *Not I*
Npm	nucleophosmin 1
Npmfl	full-length nucleophosmin 1
NpmOD	oligomerization domain of nucleophosmin 1
NpmHBD-RNABD	histone domain together with the RNA-binding domain of nucleophosmin 1
NpmRNABD	the RNA-binding domain of nucleophosmin 1
NRE	nucleolin recognition motif
NS5B	non-structural protein 5B in hepatitis C virus
N-terminus	Amino Terminus
NuLS	nucleolar localization signal
OD	oligomerization domain
Ortho-Na3VO4	Sodium orthovanadate
p	probability value
$PBS^{+/+}$	phosphate-buffered saline with magnesium and calcium
$PBS^{-/-}$	phosphate-buffered saline without magnesium and calcium
PC12	pheochromocytoma cells of rat adrenal medulla
PCR	polymerase chain reaction
PFA	paraformaldehyde
pH	potential Hydrogenii
Phe	Phenylalanine
Pre-rRNA	pre-ribosomal ribonucleic acid
RNA	ribonucleic acid
RPA	human replication protein A
rRNA	ribosomal ribonucleic acid
RRMs	RNA recognition motifs of nucleolin
RRM1	RNA recognition motif 1 of nucleolin
RRM2	RNA recognition motif 2 of nucleolin
RRM3	RNA recognition motif 3 of nucleolin
RRM4	RNA recognition motif 4 of nucleolin
SDS	sodium dodecyl sulphate
siRNA	small interfering ribonucleic acid
SOC	super optimal broth with catabolite repression media
S phase	synthesis phase
SubG1	sub-gap 1
SV40-Virus	Simian-Virus-40
TAT	transactivator of transcription
TBS	Tris-buffered saline
TBST	Tris-buffered saline with Tween 20
TAE	Tris-Acetate-EDTA buffer

Temed	Tetramethyl-ethylendiamin
TERT	telomerase reverse transcriptase
Trp	Tryptophan
TUNEL	TdT-mediated dUTP-biotin nick end labelling
U2-OS cells	osteosarcoma cells
UoC-M1	acute myeloid leukaemia cells
US11	unique short US11 glycoprotein
WT MEFs	wild-type mouse embryo fibroblasts

si units:

%	percentage
°C	degree Celsius
cm	centimetre
h	hour
l	litre
µg	microgram
µl	microlitre
µM	micromolar
M	molar
mg	milligram
min	minutes
ml	millilitre
mm	millimetre
mM	millimolar
ng	nanogram
nm	nanometre
rpm	revolutions per minute
s	seconds
Units/mg	units per milligram
V	voltage

Letter of content

1 Introduction

Nucleophosmin (B23) and nucleolin (C23) are two mainly nucleolar localized proteins (Lischwe et al., 1979) which can also shuttle between the nucleus and the cytoplasm (Borer et al., 1989). They were first found in 1973 by separating nucleolar proteins by two-dimension gel electrophoresis (Orrick et al., 1973). Highly phosphorylated forms of both proteins were found in *Novikoff hepatoma ascites tumour cells* (Olson et al., 1974). This finding led to naming nucleolin and nucleophosmin *nucleolarphosphorproteins*. Both proteins are suggested to be essential for ribosomal biogenesis (Herrera et al., 1995, Allain et al., 2000, Itahana et al., 2003), function as histone chaperones (Angelov et al., 2006, Okuwaki et al., 2001, Prinos et al., 2011), defining the localization of their binding partners (Bhat et al., 2011, Khurts et al., 2004), and transport of ribosomal proteins (Borer et al., 1989), proliferation, apoptosis and tumorigenesis (Ugrinova et al., 2007, Qin et al., 2011, Xu et al., 2012). Nucleolin has been reported to undergo a large variety of posttranslational modifications, such as phosphorylation (Schwab and Dreyer, 1997), ADP-ribosylation (Leitinger and Wesierska-Gadek, 1993), glycosylation (Galzio et al., 2012) and acetylation (Das et al., 2013). The mechanistic relationship between differential modifications, localization and functions of nucleolin is still unclear. Apart from that, the functional implication of each subdomain of nucleolin and nucleophosmin in the proliferation of the cells is also not very well understood.

1.1 Nucleolin

Nucleolin consists of 710 amino acids (100 kDa) and was first extracted from *Chinese Hamster ovary cells* nucleoli (Bugler et al., 1982). The nucleolin gene was first isolated from rat and hamster (Bourbon et al., 1988). The nucleolus consists of a *pars granulosa*, which surrounds the *pars fibrosa* and defines the periphery of the nucleolus. Nucleolin is mainly located in the *fibrillar centre* of the *pars fibrosa* of the nucleolus and also in the *fibrillar shell* enclosing the centre (Spector et al., 1984) for interacting with pre-rRNA (Ginisty et al., 1998). However, some reports doubt the localization of nucleolin in the *fibrillar centre* (Biggiogera et al., 1989). Minor amounts of nucleolin are found in the cytoplasm (Borer et al., 1989) and on the cell surface (Hovanessian et al., 2000). Nucleolin may act as a shuttle protein, while cell surface localized nucleolin acts as a ligand and transport receptor (Hovanessian et al.,

2000, Destouches et al., 2008). Nucleolin consists of an N-terminal acidic domain (50 kDa) followed by a central part with four RNA-recognition motifs (RRMs) and a glycine-arginine-rich (GAR) sequence (10 kDa) at the very end forming the C-terminus (Lapeyre et al., 1986). A variety of functions have been ascribed to these individual domains, reflecting the multifunctional character of nucleolin.

1.1.1 The N-terminus

The N-terminus (aa 1-286) of nucleolin shows evidence of nucleo-cytoplasmic shuttling by using its *nuclear localization signal* (NLS; aa 256-273) (Schmidt-Zachmann and Nigg, 1993). Interestingly, the nuclear localization of nucleolin is regulated by phosphorylation sites for the protein kinases cdc2 and CK2 within the N-terminus (Schwab and Dreyer, 1997). More precisely, nuclear localization, that takes place after dephosphorylation, and cytoplasmic localization, is dependent on nucleolin phosphorylation (Schwab and Dreyer, 1997). The nucleolar localization of nucleolin is not based on a specific signal sequence within the protein. However, the presence of the NLS sequence and, thus, nuclear transport is a prerequisite for its nucleolar localization (Schmidt-Zachmann and Nigg, 1993). In addition, the N-terminus of nucleolin encompassing four acidic-rich stretches is responsible for binding to the histone H1 and reduces chromatin condensation (Erard et al., 1988). The N-terminus can also bind to the Hdm2-RING, a protein which normally antagonizes the tumour-suppressor protein p53 (Bhatt et al., 2012). There are further serine residues which can be phosphorylated by the protein kinase CK2 (Caizergues-Ferrer et al., 1987). This leads to the conclusion that the nucleolin N-terminus has, on the one hand, mainly histone- and chromatin-binding functions and, on the other hand, shuttling functions between the cytoplasm and the nucleoplasm depending on its phosphorylation status during mitosis.

1.1.2 The RNA-binding domains

The four RNA-binding domains (also called RRMs or *RNA recognition motifs*), located in the central part and at the beginning of the C-terminus (aa 308-644), are vital for specific binding to pre-rRNA molecules and, therefore, for the ribosome biogenesis (Serin et al., 1997). These domains are commonly used sequences in diverse proteins such as nucleolin. Each of these

four RRMs of nucleolin adopts a βαββαβ-fold where two α-helices are packed against a four-stranded antiparallel β-sheet. The β-sheets can change their confirmation after binding to pre-rRNA (Ghisolfi et al., 1992b). It has been shown that RRM 1 and RRM 2 have high rRNA affinity (Serin et al., 1997) and can bind to a *nucleolin recognition element* (NRE), which is part of a pre-rRNA stem-loop, by forming a clamp and stabilizing this part of the pre-rRNA. This suggests that these two domains have chaperone functions (Allain et al., 2000). It is also possible that all four RRMs have the ability to bind to the pre-rRNA sequences called *evolutionary conserved motifs* (ECMs) to specify the pre-rRNA interaction (Ginisty et al., 2001). The RNA-binding domains can also bind to ten ribosomal proteins (Bouvet et al., 1998). Herewith, it becomes clear that the RNA-binding domains of nucleolin are essential for a correct ribosome assembly and protein biosynthesis.

1.1.3 The GAR domain

The GAR domain, first described in 1986, consists of the last 66 C-terminal amino acids of nucleolin and includes several arginine and glycine residues (Lapeyre et al., 1986). It is suggested that the domain assists the unfolding of RNA secondary structure (Ghisolfi et al., 1992a), so that the binding specificity of the RRM domains will be increased (Ghisolfi et al., 1992b). Furthermore, the GAR domain is required for ligand-binding on the cell surface and shows evidence of being involved in HIV infections (Hovanessian et al., 2000, Nisole et al., 2002, Said et al., 2002) and also hosting the hepatitis C virus NS5B through binding to its replication sequence (Kusakawa et al., 2007). The nucleolin GAR domain also binds to the tumour-suppressor protein p53, leading to an excitatory effect on its ubiquitination and degradation (Bhatt et al., 2012). It is also crucial for the co-localization of nucleolin to the nucleolus *in vivo* (Heine et al., 1993, Pellar and DiMario, 2003). Our group recently showed the interaction of the nucleolin GAR domain and the N-terminus of a protein called *fragile X mental retardation protein*, which is involved in *Fragile X Syndrome* (Taha et al., 2014). Taken all together, the GAR domain is crucial for protein and nucleic acid ligand recognition by nucleolin and most probably supporting the RRM domains in their RNA-binding activity.

1.1.4 Nucleolin and cell proliferation

The amount of nucleolin generally correlates with the proliferation rate of tumour cells and other highly proliferating cells (Derenzini et al., 1990, Storck et al., 2009). Consequently, nucleolin has been suggested as an indicator for cell proliferation (Sirri et al., 1995). In fact, nucleolin is overexpressed in stimulated *HL-60 promyelocytic leukaemia cells* (Mehes and Pajor, 1995) and shows a similar change in its expression to support melanoma growth (Mourmouras et al., 2009). In addition, the tumour cells growth can be stopped by the inhibition of cell surface-expressed nucleolin (Destouches et al., 2008, Soundararajan et al., 2009). Knockdown of the endogenous nucleolin using siRNA in *HeLa* and *DT40 chicken B lymphocyte* cells led to decreased cell proliferation and increased apoptosis (Ugrinova et al., 2007, Storck et al., 2009). Other experiments uncovered the fact that the knockdown of nucleolin also inhibits the proliferation and the growth of *human astrocytoma cells* (Xu et al., 2012). These findings lead to the conclusion that nucleolin is directly involved in tumour cell proliferation.

Nucleolin is known to interfere with the regulation of other proteins involved in cancer cell proliferation. One of them is the protooncogen Bcl2, which is known to be involved in apoptotic pathways. A decrease in nucleolin along with Bcl2 mRNA destabilization has been shown to induce apoptosis in *HL-60 leukaemia cells* (Otake et al., 2005). It was shown that nucleolin is involved in the expression of the Bcl2 gene in *CD34-positive hematopoietic cells* (Grinstein et al., 2007). In addition, the stabilization of Bcl2 mRNA was determined to be caused by an overexpression of nucleolin in *chronic lymphocytic leukaemia B-cells* (Otake et al., 2007).

Another tumour-suppressor protein is the so-called p53 protein, which induces a wide variety of repair functions in response to DNA damage, for instance, the control of translation after gamma-irradiation (Fu and Benchimol, 1997). It is also mutated in patients with the *Li-Fraumeni syndrome*, which causes different types of tumours (Malkin et al., 1990). Nucleolin is involved in up- and down-regulation of p53. An increase in cellular nucleolin leads to a reduction of p53 translation, and a decrease in cellular nucleolin induces p53 protein synthesis (Takagi et al., 2005). Taken together, these interactions show that nucleolin is a key player in the control of cell cycle, DNA repair and apoptosis.

1.2 Nucleophosmin

Nucleophosmin, which consists of 294 amino acids (37 kDa), was first isolated from rat liver nuclei (Fields et al., 1986). Its gene was isolated and characterized from both rat liver cells (Chang and Olson, 1990) and the human genome (Chan et al., 1997). Nucleophosmin is mainly located in regions of nucleolus containing rRNA, but not the *fibrillar centres* (Spector et al., 1984, Okuwaki et al., 2002). There are also reports suggesting the presence of nucleophosmin in the *dense fibrillar component* surrounding the *fibrillar centre* and the *granular component* (Biggiogera et al., 1989). Further reports suggest nucleophosmin in nucleoplasm of serum-starved *HeLa-cells* (Chan et al., 1985) and cytoplasm (Borer et al., 1989), especially at anaphase and telophase (Zatsepina et al., 1997) and in the cytoplasm of regenerative hepatocytes (Yun et al., 2003). As nucleolin, a variety of functions have also been described for nucleophosmin. These include ribosome biogenesis (Itahana et al., 2003), histone chaperone activity (Okuwaki et al., 2001) and involvement in proliferation and apoptosis (Qin et al., 2011). Nucleophosmin is a multidomain protein comprising an N-terminal oligomerization domain (13 kDa, aa 1-119) (Hingorani et al., 2000), followed by a central histone-binding domain (7 kDa, aa 120-188) and a C-terminal RNA- and DNA-binding domain (11 kDa, aa 189-294). The biologically active form of nucleophosmin seems to be a homopentameric assembly, where two of those pentamers form a decamer for binding to core histones (Dutta et al., 2001, Namboodiri et al., 2004, Lee et al., 2007).

1.2.1 The oligomerization domain

The N-terminal oligomerization domain of nucleophosmin (aa 1-119) (Hingorani et al., 2000) includes mainly nonpolar amino acids and a *nuclear export signal* (NES) at amino acid 92-104 (Wang et al., 2005, Falini et al., 2006). The oligomerization domain folds into an eight-stranded β-barrel with jellyroll topology that forms homopentameric complexes (Dutta et al., 2001, Lee et al., 2007, Okuwaki et al., 2012). A hexameric form of nucleophosmin has been proposed as a predominant and biologically active form, however, monomeric forms have also been observed (Yung and Chan, 1987). In line with the observation that the pentameric form of nucleophosmin is the active form, presence of a functional oligomerization domain seems to be critical for an aberrant cell growth in haematologic diseases (Bischof et al., 1997). Substitution of key residues responsible for nucleophosmin oligomerization (e.g. C21 with

Phe) or blockade of oligomerization interfaces using RNA aptamers, interferes with oligomerization (Prinos et al., 2011), chaperone activity (Prinos et al., 2011), induces apoptosis in cancer cells (Qi et al., 2008) and changes the subcellular localization of nucleophosmin (Jian et al., 2009). The oligomerization domain also interacts with the HIV-1 protein Rev and the HSV-1 protein US11 (Nouri et al., 2015). Taken together, these data indicate that the nucleophosmin oligomerization domain is vital for the correct function of the protein and for the survival of the cells.

1.2.2 The histone-binding domain

The central histone-binding domain of nucleophosmin (aa 120-188) contains two acidic stretches (aa 120-132 and 160-188) with an additional NLS (aa 152-157) (Hingorani et al., 2000, Okuwaki et al., 2001, Murano et al., 2008). The two acidic stretches are necessary for binding to histone H3, leading to nucleosome formation (Okuwaki et al., 2001). This interaction is dependent on acetylated forms of proteins modulating chromatin transcription (Swaminathan et al., 2005). Nucleophosmin also interacts with the linker histone H1 by the first acidic stretch of its central domain and here indirectly shows evidence of chaperone function (Gadad et al., 2011). The overexpression of nucleophosmin lacking the C-terminus (aa 120-294) revealed a dominant-negative effect on endogenous nucleophosmin concerning its histone-binding and chaperon activity (Murano et al., 2008). This mutant, furthermore, does not bind to histone H3 *in vitro* and in *293T cells* and has a dominant-negative effect on the proliferation of *293T cells* (Murano et al., 2008). The central part of nucleophosmin, especially its first acidic stretch, has ribonuclease activity, which is probably required for ribosome biogenesis (Hingorani et al., 2000). In summary, the central part of the protein is important for the binding to histones and, thus, for a correct nucleosome assembly.

1.2.3 The RNA- and DNA-binding domain

This domain of nucleophosmin is located at the C-terminal end of the protein (aa 189-294) (Wang et al., 1994, Hingorani et al., 2000). An additional NLS (aa 190-197) is embedded within the RNA- and DNA-binding domain. There is also a *nucleolar localization signal* (NuLS, aa 286 and 288) located within the C-terminal region (Nishimura et al., 2002). Cyclin

B/cdc2-mediated phosphorylation has been shown to lead to a reduced RNA-binding capacity of nucleophosmin and to its redistribution from the nucleolus into nucleoplasm and cytoplasm (Okuwaki et al., 2002). The C-terminus of nucleophosmin is mutated in about 60 % of the patients with ac*ute myeloid leukaemia* (AML), leading to its dislocation from the nucleolus to the cytoplasm (Falini et al., 2005). These mutations include the presence of an additional NES within the C-terminal domain (Nakagawa et al., 2005), loss of Trp288 and/or Trp290, and subsequent loss of nucleolar localization of nucleophosmin (Falini et al., 2006, Grummitt et al., 2008). Interestingly, the C-terminus of nucleophosmin also contains a cluster of basic amino acids (aa 188-243), which is probably an *intrinsically disordered region* (IDR). Such flexible IDRs have been described for numerous proteins as hubs for protein-nucleic-acid-interactions (Vuzman and Levy, 2012) and have recently been suggested as promising drug targets (Metallo, 2010). The cluster of basic amino acid in the C-terminus of nucleophosmin is important for binding to RNA molecules. This binding is supported through interaction with acidic stretches within the histone-binding domain mentioned above (Hisaoka et al., 2014). In addition, the RNA- and DNA-binding domain can interact with the tumour-suppressor protein p53 through its amino acids 242-269 (Lambert and Buckle, 2006). All in all, the C-terminus is important for the correct nucleolar localization of nucleophosmin. Furthermore, it plays a critical role in AML and can most probably assist ribosome assembly through its RNA-binding capacity.

1.2.4 Nucleophosmin and cell proliferation

Nucleophosmin is overexpressed in a variety of human tumours, such as hepatocellular carcinoma (Chan et al., 1989, Yun et al., 2007), colorectal carcinoma (Nozawa et al., 1996), bladder carcinoma, here associated with overexpression of nucleophosmins mRNA (Tsui et al., 2004), and thyroid tumours (Pianta et al., 2010). In addition, it can also be used as an indicator for proliferating lymphocytes (Dergunova et al., 2002). Similar to nucleolin, knockdown of nucleophosmin leads to reduced proliferation together with increased apoptosis in *human leukaemic K562 cells* (Qin et al., 2011) and *UoC-M1 leukaemic cells* (Li et al., 2005), cell cycle arrest in *HepG2 hepatoblastomacells* (Wang et al., 2011) and also G1 phase arrest in human glioma (Chen et al., 2015). Furthermore, decreased nucleophosmin mRNA levels prevent cells from entering mitosis (Jiang and Yung, 1999). These results indicate that

nucleophosmin is not only essential for the proliferation of tumour cells, but also for normal cell cycle progression.

By contrast, overexpression of nucleophosmin has antiapoptotic effects on *promyelocytic leukaemia HL-60cells* (Hsu and Yung, 2000). Similar observations have been also noted in *PC12 neuronal cells* where overexpression of nucleophosmin leads to inhibition of caspase-activated DNase (Ahn et al., 2005). Increased nucleophosmin levels also reduced p53 accumulation and, thus, apoptosis in murine mitochondria (Dhar and St Clair, 2009).

In line with the functions of nucleophosmin in proliferation and cell cycle progression, nucleophosmin antagonists have been shown to increase apoptosis of tumour cell lines. Several approaches, including antisense RNA against nucleophosmin (Liu and Yung, 1998), small molecule inhibitors of nucleophosmin oligomerization (Qi et al., 2008) and RNA aptamers (Jian et al., 2009), were employed in these studies to underline the critical role of pentameric nucleophosmin for cell proliferation.

Similar to nucleolin, many proteins influencing the cell cycle and cell proliferation have been reported to interact with nucleophosmin, and the p53 tumour-suppressor protein, mentioned above, is one of these. Nucleophosmin seems to play an ambivalent role: on the one hand, acting as a negative regulator of p53 and, thus, as an inhibitor of apoptosis (Dhar and St Clair, 2009, Li et al., 2007) and, on the other hand, acting as a p53 stabilizer (Colombo et al., 2002) by inhibiting the Hdm2-mediated p53 down-regulation (Kurki et al., 2004).

Another nucleophosmin binding protein is the nucleolar Arf, which inhibits Mdm2 and has been suggested to act as a tumour-suppressor protein. Arf is stabilized by binding to nucleophosmin (Kuo et al., 2004) and also helps to down-regulate nucleophosmin (Itahana et al., 2003), suggesting that ARF also has a negative feedback on the nucleophosmin interaction.

The nucleophosmin gene is activated by c-Myc, a protooncogene that mediates tumourigenesis (Zeller et al., 2001). C-Myc participates in the regulation of transcription of many genes involved in proliferation. Interestingly, its localization to the nucleolus arises through interaction with nucleophosmin (Li and Hann, 2013).

1.3 An intricate balance of nucleolin and nucleophosmin regulates tumour cell proliferation

As highlighted in the paragraphs above, nucleophosmin and nucleolin are involved in the proliferation of cells, their apoptosis and in cell cycle functions. The knockdown of both proteins via siRNA showed an inhibition of cancer cell proliferation. It is possible to interfere with the proliferation of tumour cells by either inhibiting the nucleophosmin oligomerization or providing a dominant negative approach by overexpressing its N-terminus. Therefore, in conclusion, both proteins are interesting targets towards an anti-tumour therapy. In addition, the involvement of nucleophosmin in hematological diseases, such as AML and *non-Hodgkin's lymphoma*, and the crucial role of nucleolin in ribosome biogenesis clearly point out that these multifaceted nucleolar proteins are key proteins, especially in the control of cell proliferation. An approach to decipher the complex role of these two multifunctional proteins in tumour cell proliferation can be overexpression of individual domains. Such a strategy would provide insights into the structure function relationship underlying the proliferative function of both proteins and, at the same time, identify the potential target sites for drug development.

Based on the information in the literature so far, we are tempted to hypothesis that: The overexpression of single nucleolin or nucleophosmin domains has dominant-negative effects on the proliferation of HeLa and Cos 7 cells in cell culture.

2 Aims

Nucleolin and nucleophosmin are two nucleolar proteins which are associated with tumorigenesis. The functional relationship between the subdomains of these multidomain proteins and the proliferation of cells still remains unclear. Unravelling the role of individual domains of these two proteins on the proliferation of cells will provide new insights into how nucleolin and nucleophosmin are involved in cancer growth and development.

The objective of this work was to identify nucleolin and nucleophosmin subdomains with dominant-negative effects on the proliferation of eukaryotic cells.

Defined subdomains of both proteins were subcloned in the pcDNA3.1flag vector. The resulting variants were transfected and overexpressed in HeLa and Cos7 cells in order to analyse the effects of the variants on proliferation.

A further aim was to define the subcellular localization of those subdomains within the cells.

3 Materials

3.1 Chemicals and Reagents

Chemical – Reagent	Company
6x DNA loading dye	Thermo Fisher Scientific Inc., Waltham, USA
10x restriction enzyme buffer	Fermentas, Waltham, USA
Ac-DEVD-AMC ALX -260-031-M005	Enzo Life Science GmbH, Lörrach, Germany
Acrylamid	Carl-Roth GmbH, Karlsruhe, Germany
Ammonium persulphate (APS)	Sigma-Aldrich Co. LLC, St. Louis, USA
Ampicillin	AppliChem, Darmstadt, Germany
Bacto-Agar	AppliChem, Darmstadt, Germany
Bacto-Trypton	BD Biosciences, San Jose, USA
Beta-Glycerolphosphat	Sigma-Aldrich Co. LLC, St. Louis, USA
Beta-Mercaptoethanol	Sigma-Aldrich Co. LLC, St. Louis, USA
Bovines Serumalbumin (BSA)	AppliChem, Darmstadt, Germany
Bradford Solution	BIO-RAD Laboratories, Hercules, USA
Bromphenole blue	Sigma-Aldrich Co. LLC, St. Louis, USA
CHAPS Detergent	Thermo Fisher Scientific Inc., Waltham, USA
ddH_2O	AG Ahmadian, Düsseldorf, Germany
DAPI mounting solution P3693	life technologies, Carlsbad, USA
Dimethyl sulphoxide (DMSO)	Sigma-Aldrich Co. LLC, St. Louis, USA
Dinatrium-Ethylendiamintetraacetat (EDTA)	MERCK, Darmstadt, Germany
Dithiothreitol (DTT)	GERBU Biotechnik, Heidelberg, Germany
dNTP Mix	Fermentas, Waltham, USA
ECL Prime Western Blotting Detection	GE Healthcare, Buckinghamshire, UK
EDTA-free inhibitor tablet	Sigma-Aldrich Co. LLC, St. Louis, USA
Ethyliumbromid	Sigma-Aldrich Co. LLC, St. Louis, USA
Gel Extraction Kit	Qiagen, Hilden, Germany
GeneRuler DNA Ladder Mix SM0331	Thermo Fisher Scientific Inc., Waltham, USA
Glucose	Carl-Roth GmbH, Karlsruhe, Germany

Glycerol	Carl-Roth GmbH, Karlsruhe, Germany
Glycine	Carl-Roth GmbH, Karlsruhe, Germany
Hydrochloride (HCL)	MERCK, Darmstadt, Germany
HEPES	Carl-Roth GmbH, Karlsruhe, Germany
Igepal CA-630	Sigma-Aldrich Co. LLC, St. Louis, USA
Magnesium Chloride (MgCl2)	MERCK, Darmstadt, Germany
NucleoBond Xtra Midi/Maxi Kit	Macherey-Nagel, Düren, Germany
Methanol	VWR, Darmstadt, Germany
Milk powder	Carl-Roth GmbH, Karlsruhe, Germany
Mini-Prep Kit	Qiagen, Hilden, Germany
Paraformaldehyd (PFA)	MERCK, Darmstadt, Germany
PCR Purification Kit	Qiagen, Hilden, Germany
Potassium Chloride (KCL)	AppliChem, Darmstadt, Germany
Phusion Buffer	Fermentas, Waltham, USA
PromegaCellTiter 96 One Solution	Promega Corporation, Madison, USA
Propidium-Iodid	Sigma-Aldrich Co. LLC, St. Louis, USA
Sodium Chloride (NaCl)	AppliChem, Darmstadt, Germany
Sodium Citrate (Na-Citrate)	MERCK, Darmstadt, Germany
Sodium dodecyl sulphate (SDS)	Carl-Roth GmbH, Karlsruhe, Germany
Sodium hydroxide (NaOH)	Sigma-Aldrich Co. LLC, St. Louis, USA
Sodium orthovanadate (Ortho-Na3VO4)	Sigma-Aldrich Co. LLC, St. Louis, USA
Spectra Low Range Protein Ladder	Thermo Fisher Scientific Inc., Waltham, USA
Sucrose	Carl-Roth GmbH, Karlsruhe, Germany
T4 DNA Ligase buffer	Fermentas, Waltham, USA
Tetramethylethylendiamin (Temed)	Carl-Roth GmbH, Karlsruhe, Germany
Tricine	Sigma-Aldrich Co. LLC, St. Louis, USA
Tris	Carl-Roth GmbH, Karlsruhe, Germany
Tris-HCL	Carl-Roth GmbH, Karlsruhe, Germany
Triton x 100	MERCK, Darmstadt, Germany
Trypanblue 0.4 %	BIO-RAD Laboratories, Hercules, USA
TurboFect Transfection Reagent	Thermo Fisher Scientific Inc., Waltham, USA
Tween 20	Sigma-Aldrich Co. LLC, St. Louis, USA

Yeast Extract	Carl-Roth GmbH, Karlsruhe, Germany

3.2 Enzymes

Enzyme	Company
Bam HI restriction enzyme	Fermentas, Waltham, USA
Fast AP	Fermentas, Waltham, USA
Not I restriction enzyme	Fermentas, Waltham, USA
Phusion Polymerase	Fermentas, Waltham, USA
T4 DNA Ligase	Fermentas, Waltham, USA

3.3 Machines and Softwares

Machine – Software	Company
Automatic cell counter TC 20	Bio-Rad Laboratories, Hercules, USA
BD CellQuest Pro software	BD Biosciences, San Jose, USA
Carl Zeiss Axiovert 25	Zeiss, Jena, Germany
Electrophoresis Chambers	Bio-Rad Laboratories, Hercules, USA
EPS Power Supplies 600	GE Healthcare Life Science, Freiburg, Germany
Eppendorf Bio Photometer plus	Eppendorf GmbH, Wesseling-Berzdorf, Germany
Eppendorf centrifuge 5810R	Eppendorf GmbH, Wesseling-Berzdorf, Germany
Eppendorf centrifuge 5417R	Eppendorf GmbH, Wesseling-Berzdorf, Germany
Eppendorf Mastercycle	Eppendorf GmbH, Wesseling-Berzdorf, Germany
FACS Calibur	BD Biosciences, San Jose, USA
GraphPad Prism 5 Version 5.04	GraphPad Software Inc., La Jolla, USA
Hera freeze -80 °C	Heraeus Holding GmbH, Hanau, Germany
Heracell 150 CO_2 Incubator	Heraeus Holding GmbH, Hanau, Germany
Heraeus instruments Labofuge 400 P	Heraeus Holding GmbH, Hanau, Germany
Hera Safe cell culture bench	Heraeus Holding GmbH, Hanau, Germany
Hettich Universal 30F	Gemini bv, Apeldoorn, Netherlands
INTAS imaging chemo camera	INTAS Science Imaging Instruments, Göttingen, Germany
Lauda Aqualine AL 25	Lauda Dr. R. Wobser GmbH, Lauda-Königshofen, Germany
LSM510-Meta confocal microscope	Zeiss, Jena, Germany
Mini Trans-Blot Cell	Bio-Rad Laboratories, Hercules, USA
Nanodrop	Thermo Fisher Scientific Inc., Waltham, USA
Nikon TE2000 fluorescence microscope	Nikon Instruments Europe BV, Amsterdam, Netherlands
Shaker WS5	Edmund Bühler GmbH, Hechingen, Germany
TECAN Infinite M 200 microplate reader	Tecan Trading AG, Männedorf, Switzerland
TECAN I control software	Tecan Trading AG, Männedorf, Switzerland
UV Table	Bio Budget Technologies GmbH, Krefeld, Germany

3.4 Oligonucleotides

Primers	Sequences
Nclflfw(1-710)	5'- TAATAAGGATCCATGGTGAAGCTCGCGAAGGCAGGT-3'
Nclflrev(1-710)	3'- TAATAAGCGGCCGCCTATTCAAACTTCGTCTTCTTTCC-5'
NclN-Termrev(1-297)	3'- TAATAAGCGGCCGCCTATTTCTGTTTCTTGGCTTCAGGAGC-5'
NclN-TermRRM1rev(1-381)	3'- TAATAAGCGGCCGCCTATGGTTTCTCTAGTTTAATTTC -5'
NclRRM14GARfw(273-710)	5'- TAATAAGGATCCGTCAAAGAAGCACCTGGAAAACG-3'
NclRRM12fw(273-466)	5'- TAATAAGGATCCGTCAAAGAAGCACCTGGAAAACGA-3'
NclRRM12rev(273-466)	3'- TAATAAGCGGCCGCCTACTCTCCAGTATAGTACAG -5'
NclRRM34fw(467-644)	5'- TAATAAGGATCCGGTCAAAATCAAGACTATAGAGGT-3'
NclRRM34rev(467-644)	3'- TAATAAGCGGCCGCCTACCAGTCCAAGGTAACTTT-5'
NclRRM4GARfw(499-710)	5'- TAATAAGGATCCACTCTGTTTGTCAAAGGCCTG-3'
NclGARfw(645-710)	5'- TAATAAGGATCCAAACCTAAGGGTGAAGGTGGC-3'
Npmflfw(1-294)	5'- TAATAAGGATCC G ATG GAA GAT TCG ATG GAC ATG-3'
Npmflrev(1-294)	3'- TAATAAGCGGCCGC AAG AGA CTT CCT CCA CTG CCA-5'
NpmODrev(1-122)	3'- TAATAAGCGGCCGCTTAATCTTCCTCCACAGCTACTAAG-5'
NpmHBD-RNABDfw(123-294)	5'- TAATAAGGATCC AAG AGA CTT CCT CCA CTG CCA-3'
NpmRNABDfw(241-294)	5'- TAATAAGGATCCAGTTCTGTAGAAGACATTAAA-3'

From Eurofins Genomics, Ebersberg, Germany

3.5 Antibodies

Antibodies for Immunoblot

Primary Antibody	Company
Anti-Flag mouse F3165	Sigma Aldrich Co. LLC, St. Louis, USA
Anti-Npm mouse ab10530	abcam, Cambridge, UK
Anti-Ncl rabbit ab22758	abcam, Cambridge, UK
Anti-α-tubulin rat SM568	Acris Antibodies GmbH, Herford, Germany

Secondary Antibody	Company
Anti-mouse in rabbit P0161	Dako Deutschland GmbH, Hamburg, Germany
Anti-rabbit 7074P2	Cell Signaling Technology, Cambridge, UK
Anti-rat ab7010,	abcam, Cambridge, UK

Antibodies for Confocal laser scanning microscopy

Primary Antibody	Company
Anti-Flag mouse F3165	Sigma Aldrich, Co. LLC, St. Louis, USA
Anti-Ncl rabbit ab22758	abcam, Cambridge, UK
Alexa Fluor®546 Phalloidin	life technologies, Carlsbad, USA

Secondary Antibody	Company
Alexa Fluor®488 Goat Anti-rabbit	life technologies, Carlsbad, USA
Alexa Fluor®488 Goat Anti-mouse	life technologies, Carlsbad, USA
Alexa Fluor®633 Goat Anti-rabbit	life technologies, Carlsbad, USA
Alexa Fluor®633 Goat Anti-mouse	life technologies, Carlsbad, USA

3.6 Cell Culture

Supply	Company
6-well plates, 96-well plates	TPP Techno Plastic Products AG, Trasadingen, Switzerland
10 cm cell dish,	TPP Techno Plastic Products AG, Trasadingen, Switzerland
20 µl, 10 µl pipette	Eppendorf GmbH, Wesseling-Berzdorf, Germany
25 ml, 10 ml, 5 ml pipette	TPP Techno Plastic Products AG, Trasadingen, Switzerland
1000 µl, 200 µl pipette,	Eppendorf GmbH, Wesseling-Berzdorf, Germany
Cos-7 cells	The Leibniz Institute DSMZ, Braunschweig, Germany
counting slides	Bio-Rad Laboratories, Hercules, USA
cover-slips 18 mm	VWR, Darmstadt, Germany
DMEM Media	Gibco life technologies, Carlsbad, USA
Eppendorf Tubes 5 ml	Eppendorf GmbH, Wesseling-Berzdorf, Germany
FACS BD Falcon	BD Biosciences, San Jose, USA
Falcon tubes 50 ml, 15 ml	Sigma Aldrich Co. LLC, St. Louis, USA
Fetal bovine calf serum	Gibco life technologies, Carlsbad, USA
HeLa cells	The Leibniz Institute DSMZ, Braunschweig, Germany
Object glasses	NeoLab, Heidelberg, Germany
PBS (10 x) with Mg^{2+} and Ca^{2+}	Genaxxon bioscience GmbH, Ulm, Germany
PBS (10 x) without Mg^{2+} and Ca^{2+}	Genaxxon bioscience GmbH, Ulm, Germany
Penicillin and Streptomycin	Gibco life technologies, Carlsbad, USA
Trypsin-EDTA solution	Sigma-Aldrich Co. LLC, St. Louis, USA
T150 flask, T75 flask	Thermo Fisher Scientific Inc., Waltham, USA

3.7 Further Supply

Supply	Company
Amersham Hybond ECL nitrocellulose membrane	GE Healthcare, Buckinghamshire, UK
Ncl and Npm template in pGEX-4T-1vector	Provided by (Yang et al., 2002)
pcDNA3.1flag vector	Invitrogen life science, Waltham, USA
Whatman blotting papers	Sigma Aldrich Co. LLC, St. Louis, USA

3.8 Mastermix

Polymerase chain reaction

Mastermix	20 µl 5x Phusion Buffer 1 µl DMSO 1 µl dNTP Mix 74.9 µl ddH_2O 0.3 µl forward primer 0.3 µl reverse primer 1 µl DNA template Ncl or Npm
Enzyme	1.5 µl Phusion Polymerase

Digestion of variants

Mastermix	1-5 µg DNA 16 µl ddH_2O 3 µl 10x buffer
Enzyme	1.5 µl Bam HI 1.5 µl Not I 1.5 µl Fast AP

Ligation of plasmid

Mastermix	100 ng DNA 3.3 µl pcDNA3.1 flag vector 2 µl T4 DNA Ligase buffer 3.7 µl ddH_2O
Enzyme	1.5 µl T4 DNA Ligase

3.9 Media

LB Media 1l	10 g Bacto-Trypton 5 g Yeast Extract 10 g NaCl ddH_2O to 1 l 1 ml ampicillin
SOC-Media 1l	20 g Bacto-Trypton 5 g Yeast Extract 2 ml of 5 M NaCl 2.5 ml of 1 M KCl 10 ml of 1 M $MgCl_2$ 20 ml of 1 M Glucose
Ampicillin Plates	1l LB Media with ampicillin 16 g Bacto-Agar

3.10 Buffer and Gel

Electrophoresis

TAE-Buffer 1 %	2 M Tris 50 mM EDTA pH 8.5
1 % Agarose gel	3 g Agar 297 ml TEA-Buffer 1 % 3 µl Ethyliumbromid

Fish Buffer

Mastermix	50 mM Tris-HCL 100 mM NaCl 2 mM $MgCl_2$ 1 % Igepal CA-630 10 % Glycerol 20 mM beta-glycerol 1 mM Ortho-Na_3VO_4 1 EDTA-free inhibitor tablet

Laemmli Buffer 5x

Mastermix	50 mM Tris/HCl 50 % Glycerol 5 % Beta-Mercaptoethanol 10 % SDS 0.5 % Bromphenole blue

SDS-PAGE

10 % APS	5 g APS 50 ml ddH_2O
3x gel buffer	181.5 g Tris HCL to pH 8.45; 1.5 g SDS ddH_2O to 500 ml
10x lower buffer	121 g Tris 121 g 12N HCL to pH 8.9 ddH_2O to 500 ml;
10x upper buffer	60.5 g Tris 89.6 g Tricine 89.6 g 5.0 g SDS ddH_2O to 500 ml;
Resolving Gel	1.4 ml ddH_2O 0.6 ml 80 % glycerol 2 ml 3x gel buffer 2 ml 30 % acrylamid 45 µl APS 15 µl Temed
Stacking Gel	1.5 ml ddH_2O 0.6 ml 3x gel buffer 0.3 ml 30 % acrylamid 20 µl 10 % APS 10 µl Temed
Transfer buffer 10x 1l	30.3 g Tris 144.1 g Glycine ddH_2O up to 1l
Transfer buffer 1x 1l	100 ml Transferbuffer 10x 200 ml Methanol ddH_2O up to 1l

Immunoblot

TBST 10x 1l	30 g Tris 80 g NaCl 2 g KCL 5 ml Tween 20

	ddH_2O to 1l
TBS 10x 1l	30 g Tris 80 g NaCl 2 g KCL ddH_2O up to 1l
Milk	2.5 g Milk powder TBST 1X up to 50ml

Nikoletti assay

Reaction buffer	1250 µl Propidium-Iodid 891 µl Na-Citrate 50 µl Triton X 100 50 ml ddH_2O

Caspase 3 assay

Reaction buffer	50 mM HEPES pH 7.3 100 mM NaCl 10 % Sucrose 0.1 % CHAPS 10 mM DTT 50 µM Ac-DEVD-AMC

Confocal laser scanning microscopy

0.25 % Triton x 100	100 ml PBS without Mg^{2+} and Ca^{2+} 250 µl Triton x 100
3 % BSA	1.5 g BSA 50 ml 0.25 % Triton x 100
1 % BSA	16 ml 3 % BSA 33.33 ml 0.25 % Triton x 100
Paraformaldehyd (PFA)	4 g PFA 86 ml ddH_2O heating up to 70.°C while stirring 3 drops 5 M NaOH cooling down the solution 10 ml PBS (10 x)

4 Methods

4.1 Cloning of plasmids

Full-length nucleolin (Nclfl, 1-710), the N-terminus (NclN-Term,1-297), the N-terminus and the RNA-binding domain 1 (NclN-TermRRM1, 1-381), the C-terminus (NclRRM14GAR, 273-710), the RNA-binding domain 1 and 2 (NclRRM12, 273-466), the RNA-binding domain 3 and 4 (NclRRM34, 467-644), the RNA-binding domain together with the GAR domain (NclRRM4GAR, 499-710), and the GAR domain (NclGAR, 645-710) of nucleolin, the full-length nucleophosmin 1 (Npmfl, 1-294), the oligomerization domain (NpmOD, 1-122), the histone together with the RNA-binding domain (NpmHBD-RNABD, 123-294), and the RNA-binding domain (NpmRNABD, 241-294) of nucleophosmin 1 were amplified by standard PCR methods (compare Figure 1). The resulting PCR products were cloned into the pcDNA3.1 flag vector via *Bam HI* and *Not I* restriction sites. The sequences of all plasmids generated correctly were, subsequently, confirmed via Sanger sequencing.

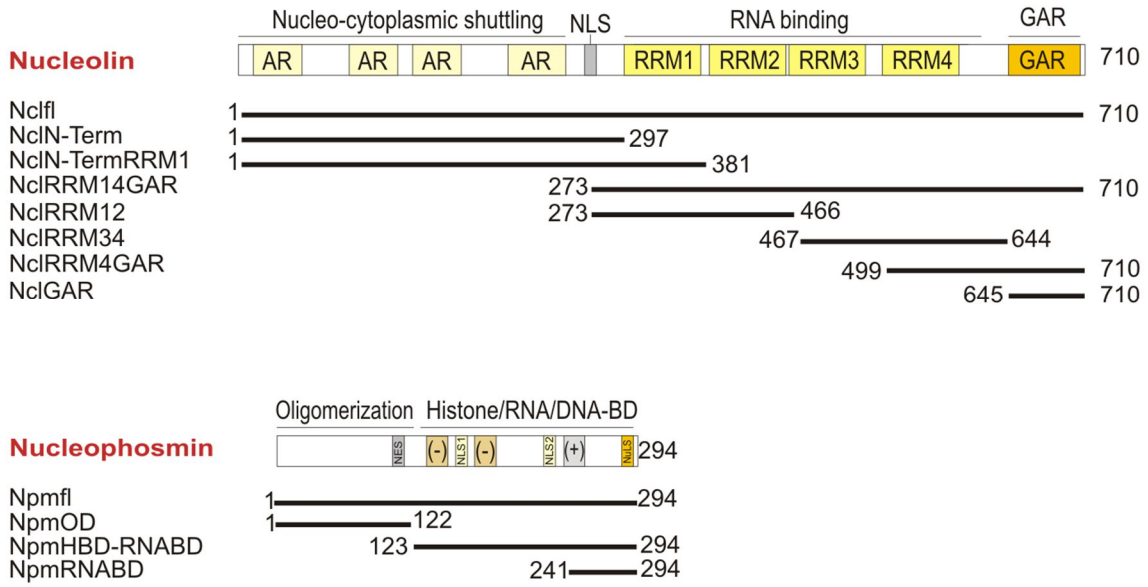

Figure 1: Defined Ncl and Npm variants. 12 Different variants of the Ncl and Npm protein were generated *via* polymerase chain reaction (PCR); AR: Acidic Regions; NLS: Nuclear localization signal; RRM: RNA recognition motif; GAR: glycine-arginine-rich domain; NES: Nuclear export signal; NuLS: Nucleolar localization signal; (-): acidic regions; (+): basic region; Histone/RNA/DNA-BD: Histone/RNA/DNA-Binding domain.

4.1.1 Polymerase Chain Reaction

Polymerase chain reaction (PCR) is a method used to amplify DNA sequences out of a template DNA for further cloning steps. It is based on the activity of a specific enzyme called DNA polymerase, which is temperature-dependent and can reproduce the template by using several components (Mullis and Faloona, 1987). The reaction preparation was always based on 100 µl volume containing 20 µl 5x buffer, 1 µl DMSO, 1 µl dNTP Mix, 1.5 µl Phusion enzyme (polymerase), 1 µl DNA template, 74.9 µl ddH_2O, 0.3 µl forward primer and 0.3 µl reverse primer. The reaction starts with a denaturation of the template DNA at high temperature (> 98 °C) resulting in single-stranded DNA. Reduction of the temperature below the annealing temperature allows specific oligonucleotide primers to anneal to complementary sequences of the single-stranded template DNA. Next, the temperature is increased to the optimal working temperature of the DNA polymerase, which, in turn, can elongate the primers complementary to the template strand by adding nucleotides (dNTP). Multiple cycles of denaturing, annealing and elongation are performed throughout the PCR reaction so that the DNA is amplified exponentially. The PCR was carried out in an Eppendorf mastercycle (Eppendorf, Germany).

Standard PCR Programme

98 °C	30 s	Initial	
98 °C	10 s	Denaturing	
Tm -5 °C	10 s	Annealing	x 35
72 °C	15-30 s/kb	Elongation	
72 °C	5 min	Final Elongation	

4.1.2 Gel Electrophoresis

Electrophoresis is a method in which samples containing molecules, for example, PCR samples, are loaded onto an agarose gel. The samples then migrate through the gel covered with 1 % TEA buffer for approximately 25 min due to an added tension of 100 V and the fragments containing DNA are separated from each other depending on their size and charge. Ethidium bromide within the agarose gel intercalates with the DNA and the band can then be visualized under a photochemical camera. Here, the size of the band can be compared with a loaded marker running parallel to the bands. The so-called “analytical gel” is used as a control

if the PCR samples have the correct size. The PCR products were separated from PCR components, including primers and salt, on preparative gels. The PCR products were isolated from the gels using a commercial *Gel extraction kit* (QIAGEN, Hilden), according to the manufacturer's instructions.

4.1.3 Digestion of variants

Following gel extraction, the PCR products were digested by so-called restriction enzymes for later ligation with the pcDNA3.1 flag vector used to transfect mammalian cell lines.

The pcDNA3.1 vector is FLAG-tagged for subsequent immunoblotting and confocal microscopy experiments. The FLAG-tag is a short sequence of eight amino acids which can be detected in the cell or cell lysate by the corresponding FLAG-tag antibody and is well-known to avoid later interaction or disturbance within the cell and its function.

Restriction enzymes originally belong to bacteria and are used as a defence mechanism. Nowadays, they are a useful tool for cloning DNA constructs. An amount of 1 – 5 µg of DNA were digested with *Bam HI* for 1.5 h at 37 °C. After this step, the sample was cleaned, according to the protocol of the *Qiagen PCR Purification Kit*. The remainder of the purified DNA was used for another digestion step using the *Not I* restriction enzyme so that the DNA fragment was cleaved from both sides, followed again by a cleaning step using the *Qiagen PCR Purification Kit*. Both enzymes cut the double DNA strand between specific base pairs (bps). The cutting site is included in the designed primer sequence, which represents the beginning of each construct. The pcDNA3.1 flag vector was digested with *Bam HI* and *Not I* analogous to the PCR products. However, an additional dephosphorylation step of 30 min at 37 °C using *FastAP* was carried out for the preparation of the linearized vectors. This step reduces the probability of vector self-ligation. Following digestion and dephosphorylation, the linearized pcDNA3.1 flag vector was purified using the *Qiagen PCR Purification Kit* mentioned above. The result is a double-sided sticky end-cleaved DNA fragment ready to be ligated with the similarly cleaved multiple cloning side of the vector.

4.1.4 Ligation of plasmid

The cleaved DNA constructs and the cleaved vector were ligated. For ligation, 100 ng of vector were ligated for 2 h at room temperature in a 3:1 or 5:1 molar ratio with the corresponding PCR products using *T4 DNA ligase*. The result is a pcDNA3.1 flag vector

containing the target DNA at its multiple cloning site. After this step, the sample needed to be heated up to 72 °C for 5 min to inactivate the ligase for further steps. This step is followed by a cleaning step using the *Qiagen PCR Purification Kit*

4.1.5 Electric transformation

Electric transformation is a method used to transfer extracellular material, such as DNA, into bacteria cells by applying high voltages. Therefore, 5 µl of ligation product and 45 µl of *Escherichia coli XL1 blue* electrocompetent bacteria cells were mixed in an electroporation cuvette and high voltages were applied. This results in the vector passing through the bacteria membrane (Neumann et al., 1982). After this step, bacteria containing the vector needed to recover from the electroporation. Therefore, they were transferred from the cuvette to 1 ml SOC media and gently shaken at 37 °C for 1 h.

4.1.6 Plasmid amplification

In order to distinguish between *E. coli XL1 blue* bacteria cells containing the vector with the desired DNA and those which do not, 100 µl of bacteria grown in 1 ml SOC media were transferred to a 10 cm LB media agar plate containing ampicillin. Agar plates were incubated at 37 °C for 12 h. The pcDNA3.1 flag vector contains an ampicillin-resistant gene on its multiple cloning site. As a consequence, only colonies containing the transferred plasmid can grow. For the next step, a single colony was picked from the agar plate using a pipette tip. This colony containing the vector with the desired gene was amplified by incubation in a 50 ml Falcon tube containing 5 ml LB media and 5 µl ampicillin, and gently shaken for 12 h at 37 °C.

4.1.7 DNA extraction of plasmids

DNA was extracted from the 5 ml bacteria culture, according to the protocol of the *Qiagen Mini-Prep Kit*. Before extracting the DNA, a glycerol backup stock was prepared from the culture by using 750 µl grown cultures and 750 µl sterile glycerol, which was then frozen at -80 °C. Following plasmid isolation, the DNA concentration was measured by detection of the absorbance at 260 nm using a *Thermo Scientific nanodrop*, making sure that the absorbance at A260/280 lies at~ 1.8, which is accepted as pure for DNA. The DNA was also loaded on agarose gel to control the purity of the band after running a gel electrophoresis. The DNA extracted was sent for sequencing to verify the DNA sequence accuracy.

4.1.8 MIDI preparation of plasmids

A number of 100 ml cultures containing LB media and ampicillin were inoculated from glycerol stocks to obtain more DNA suitable for the transfection of mammalian cell lines. The DNA was extracted according to the protocol of the *Nucleobond Xtra Midi/Maxi Kit.*

4.2 Cell culture

HeLa cells and Cos-7 cells were grown at 37 °C and 5 % CO_2 in DMEM 1 % glucose and 1 % pyruvat media supplemented with 10 % fetal calf serum and 1 % penicillin/streptomycin ($DMEM^{+/+}$). Cos-7 cells are fibroblast-like green monkey kidney cells and are transformed with SV40. They are well-known for an efficient transient transfection. HeLa cells are uterus-derived human tumour cells and are used to verify results in a human cell system. Both cell lines were treated in the same way in the following steps.

4.2.1 Seeding of cells

After two days of culturing, the DMEM media was discarded and the cells were washed with PBS without calcium and magnesium ($PBS^{-/-}$). An amount of 3 ml $PBS^{-/-}$ containing 10 % Trypsin was added to the cells and incubated at 37 °C for 5 min. After all the cells were detached, 9 ml $DMEM^{+/+}$ was added to the cells to neutralize the Trypsin and to wash the cells from the dish. The cells were collected in a 50 ml Falcon tube now containing cells, Trypsin and media. The tube was centrifuged at 1200 rpm for 5 min (Heraeus instruments Function line Labofuge 400 P, Thermo Fisher Scientific). The cell pellet was resuspended in fresh $DMEM^{+/+}$ media. The cells were counted in an automatic cell counter by using 10 µl of resuspended cells and 10 µl of trypan blue (Bio-Rad Laboratories). The Cos-7 cells (1×10^6) or HeLa cells (1×10^6) were seeded into a new T75 flask for transient transfection.

4.2.2 Transient transfection of cells

Transient transfection of cells is a method by which foreign plasmids containing the desired DNA are delivered into cells with the aim of studying its effects on defined aspects. The transfection is not steady, which means the DNA is not integrated into the genome, but usually remains long enough in the cell to receive various copies of the DNA, protein synthesis and related biological responses (Graham and van der Eb, 1973). A variety of

methods, such as viral transfection, calcium phosphate, liposome fusion, polycations, electroporation, microinjection and protoplast fusion, are known for transient transfection. The transfection was performed according to a combination of the polycations and liposome fusion methods which leads to cationic lipids surrounding the DNA being delivered into the cell (Felgner et al., 1987). *TurboFect Transfection Reagent* derived by *Thermo Scientific* is a lipid-based cationic polymer known for forming positively-charged complexes with the plasmid containing the DNA desired. This complex interferes with the negatively-charged cell membrane and is taken up by the cell using endocytosis. Two main benefits, the high transfection efficiency and the low cytotoxicity, recommend the use of this reagent.

4.2.3 Transfection to 10 cm dish

Cells were transfected by using the *Thermo Scientific TurboFect Transfection Reagent*. The cells (1.3×10^6) were seeded 16 h before transfection onto a 10 cm dish containing 10 ml of $DMEM^{+/+}$media. The next day, 5 µg of DNA, 1 ml of DMEM without fetal calf serum and antibiotics ($DMEM^{-/-}$), and 10 µl of *TurboFect Transfection Reagent* were mixed and briefly vortexed. After an incubation time of 20 min, the mixture was added directly to the cells. The dish was gently rocked to achieve an even distribution of the mixture. Six hours after incubation, the media was changed to fresh $DMEM^{+/+}$ media. The incubation cells were harvested 48 h afterwards, and used for further analysis. The same protocol was used for the transfection of 6-well and 96-well plates using the following concentrations.

4.2.4 Transfection of 6-well plates

The cells (1×10^5) were seeded in 1 ml DMEM medium containing 10 % fetal calf serum and 1 % Penicillin/Streptomycin using 1 µg DNA with 200 µl DMEM media without fetal calf serum and antibiotics and 2 µl *TurboFect*.

4.2.5 Transfection of 96-well plates

Two thousand cells were seeded in 200 µl of DMEM media containing 10 % fetal calf serum and 1 % Penicillin/Streptomycin using 0.2 µg DNA with 20 µl DMEM media without fetal calf serum and antibiotics and 0.4 µl *TurboFect*.

4.3 Protein analysis

4.3.1 Preparing samples for SDS-PAGE and immunoblot

Transfected cells on a 10 cm dish were washed with $PBS^{-/-}$ and then lysed directly by using 250 µl of lysis buffer (fish buffer) containing 50 mM Tris-HCL, 100 mM NaCl, 2 mM MgCl2, 1 % Igepal CA-630, 10 % Glycerol, 20 mM beta-glycerolphosphat, 1 mM Ortho-Na3VO4 and 1 EDTA-free inhibitor tablet. Cell lysates were collected in 1.5 ml tubes and centrifuged at 14,000 rpm for 2 min. The supernatant was taken and the protein concentration was determined using the Bradford Assay. For the Bradford assay, 2 µl of sample were mixed with 500 µl of Bradford Solution. Protein concentration was determined by measuring the adsorption of this mixture between 465 nm and 595 nm. The adsorption at 595 nm should lie between 0.2 and 0.8 to enable the linear measurement. The samples were all adjusted to the same concentration of protein by using this method and the dilution with ddH_2O and 5x Laemmli buffer.

4.3.2 SDS-PAGE

The SDS-PAGE is a polyacrylamid gel electrophoresis used to separate the loaded samples, including proteins, concerning their molecular weight. Before being loaded onto the SDS-PAGE, samples are mixed with 5x Laemmli buffer and heated up to 95 °C for 5 min with the aim of denaturing the proteins contained. Laemmli buffer consists of Beta-mercaptoethanol, which breaks disulphide bonds, and SDS, which breaks hydrogen bonds, binds to amino acids and causes a negative charged protein able to run through the gel from the anode to the cathode (Laemmli, 1970). Depending on the molecular weight, larger proteins run slower and smaller proteins run faster through the gel. In addition, the running speed depends on the charge given by amino acids in the protein. The acryl amide concentration of the gels was adjusted depending on the molecular weight of the samples. The gel usually runs at 80 V for 2 h and is stacked in a specific cassette including a 1x lower and 1x upper reservoir buffer.

4.3.3 Immunoblotting

Immunoblotting is a sensitive method for protein detection. Proteins are transferred (blotted) from an SDS-PAGE onto a nitrocellulose membrane (Towbin et al., 1979). Transfer of proteins from an acrylamide gel to a membrane immobilizes proteins in a specific position corresponding to their prior position in the acrylamide gel. Immunoblotting was performed at

a voltage of 100 V for 60 min. Visualization of proteins on the membrane is carried out by using a specific antibody. Therefore, the membrane needs to be blocked with 5 ml of milk for 60 min and then incubated with a primary antibody, according to the manufacturer's instructions. Following incubation with primary antibody, the membranes were washed three times for 10 min with 10 ml TBST 1x. This procedure was repeated for the secondary antibody, followed by an additional washing step of 10 ml TBS 1x for 10 min at the end. Each washing and incubation step was performed with a shaker to achieve an even distribution of the sample. The secondary antibody and, subsequently, the target protein were visualized by using 1 ml ECL based chemiluminescence under a photochemical camera

4.4 Proliferation assay

4.4.1 MTT assay

The MTT assay is a method to measure cell viability, proliferation and cytotoxicity. It is based on the bioreduction of the salt 3-(4,5-dimethylthiazol-2-yl)-2,5-diphenyl tetrazolium bromide to formazan (Mosmann, 1983). This reaction is carried out by dehydrogenases using NADPH or NADH. The amount of formazan is measured by the absorbance at 560 nm and is a direct indicator of mitochondrial activity and the amount of living cells.

4.4.2 Procedure for the MTT assay

An amount of 40 µl of *PromegaCellTiter 96 One Solution Reagent* was added to cells grown and transfected in triplicate on 96-well plates. The excitation wavelength was measured at 560 nm using the *TECAN infinite M 200 microplate reader* and the *TECAN I control software* immediately after adding the solution. After this step, cells were incubated at 37 °C and 5 % CO_2 for 20 min. The measurements were repeated three more times with 20 min of incubation in between for each step. The first measurement immediately after 0 min was subtracted from each of the following three measurements.

4.5 Fluorescence-activated cell sorting (FACS)

4.5.1 FACS analysis

Fluorescence activated cell sorters were first established by Fulwyler (Fulwyler, 1965). The method is based on the idea of sorting a certain amount of cells concerning their content of DNA or RNA, cell volume, cell surface antigens or enzymatic activity. There are several more parameters that can be investigated. Single cells are entered into the machine before passing a laser signal. This laser measures the fluorescence intensity of single cells related to the aim of study. Therefore, cells need to be pretreated with a fluorophore attached to an antibody or chemical, aiming a structure in or on the cell. After measuring the fluorescence intensity, cells can be sorted by added charges, depending on the outcome of the intensity measured.

4.5.2 Nikoletti assay

The Nikoletti assay is a commonly used method for analysing the distribution of the cells in different cell cycle phases. The DNA of the cells is stained by propidium-iodide, which works as a fluorophore and can be read out by the FACS. Each cell contains a specific amount of stained DNA depending on the current cell cycle phase, which makes it possible to distinguish between Sub-G1 (Apoptosis or Necrosis), G0/G1 phase, S phase, G2/M phase and multinucleate cells (Nicoletti et al., 1991).

4.5.3 Procedure for the Nikoletti assay

The cells were grown and transfected on 6-well plates. Media was collected in a FACS tube. The cells were washed with 1 ml $PBS^{-/-}$ (also collected). They were detached with 500 µl trypsine and resuspended in 1 ml $DMEM^{+/+}$ (also collected). The FACS tube was centrifuged at 1000 rpm at 4 °C for 8 min. The supernatant was discarded and the cells were resuspended in 1 ml $PBS^{-/-}$. The cells were pelleted again by centrifugation (as previously) and the supernatant was discarded. The cells were resuspended in 150 µl Nicoletti solution (containing Triton X 100 and sodium-citrate for permeabilizing the cells and propidium-iodide for staining their DNA) while vortexing and then incubated in a 4 °C cold room for 2 h. The FACS data was analysed using *BD CellQuest Pro software*.

4.6 Caspase 3 assay

4.6.1 Caspase 3

Caspase 3 is a cell protease involved in the apoptosis of cells and the correct development of organisms. Apoptosis is the programmed cell death and an important mechanism after cells undergo certain fail functions through internal or external damage. After cell damage, caspase 3 is activated and, for example, cleaves specific proteins, such as laminin, which is important for the internal cytoskeleton and the shape of the cell. Furthermore, it is important for chromatin condensation and DNA fragmentation. Caspase 3 cleaves the protein's C-terminal of aspartate residues (Gurtu et al., 1997).

4.6.2 Procedure for the caspase 3 assay

The caspase 3 assay is based on the substrate DEVD, a short amino acid sequence (aspartate, glutamate, valin, aspartate) which is linked to a fluorophore (AMC = 7-Amino-4-methylcumarin) and is added to the sample of interest. Caspase 3 cleaves the DEVD substrate and releases the fluorophore. The amount of fluorophore can be measured and is a direct indicator of the activity of caspase 3 and apoptosis within the sample. The cells and their media, 48 h post transfection on 10 cm dishes, were collected in a 50 ml Falcon tube. The cells were resuspended and washed three times in 1 ml $PBS^{-/-}$ and then lysed in 100 µl fish buffer. The cell lysates were centrifuged at 4 °C for 10 min to aliquot the supernatant into an extra tube and measure the protein concentration. An amount of 50 µg of the sample was mixed with 50 µl fish buffer and then aliquoted on a 96-well plate in 150 µl reaction buffer containing 50 mM HEPES pH 7.3, 100 mM NaCl, 10 % Sucrose, 0.1 % CHAPS, and, additionally, shortly before the measurement, 10 mM DTT and 50 µM Ac-DEVD-AMC to start the reaction. The fluorophore concentration of the DEVD cleaving activity then was read out by the *TECAN Infinite M 200 microplate reader* using the *TECAN I control software*. Analyses were carried out at 10 min intervals for a total of 3 h at 37 °C and an emission wavelength of 442 nm. A measurement of a sample only containing fish buffer was subtracted from the last measurement after 3h for each variant. The read-out for the DEVD cleaving activity was performed by the laboratory for molecular radiooncology (Prof. Dr. Reiner Jänicke) of the Heinrich-Heine-University in Düsseldorf, Germany.

4.7 Confocal laser scanning microscopy (CLSM)

4.7.1 CLSM analysis

The CLSM uses a specific microscope to visualize fluorescence signals emitted by cells or tissue compartments (LSM510-Meta confocal microscope, Zeiss, Jena, Germany). The cells were labelled with fluorescent antibodies, as described in the immunoblotting section of this thesis. This fluorescence microscopy cannot provide a total observation of the whole cell at one time, but provides a snapshot of one cell layer. Analysis of multiple layers of the cells later allows reconstruction of the whole sample using a computer programme. The key idea of this method is the confocal observation of the sample, which refers to the fact that the spot observed on the sample is in focus together with the reflected light from this spot within the light shade right before the detector simultaneously. Herewith, it is possible to reach a high contrast by depressing spread out light from the object. The emitted or reflected light passes a so-called pinhole with a specific diameter which is adjusted once at the beginning and should not be changed throughout the experiment. Since normal light is not a sufficient animator for fluorescence signals, the CLSM uses lasers of different wavelengths. Three different wavelengths were used for the following experiment: 488 nm for the anti-flag antibody used to visualize nucleolin or nucleophosmin variants, 633 nm for the endogenous localized nucleolin antibody and 546 nm for Phalloidin to visualize the cytoskeleton of the cell. A mounting solution was used for fixing cover-slips with transfected cells on an object glass. Furthermore, the mounting solution contains a DAPI signal to visualize the cell nucleus of transfected cells at a wavelength of 385 nm.

4.7.2 Procedure for the CLSM

The cells were seeded, cultured and transfected on 6-well plates containing one 18 mm cover-slip per well. The medium was removed 48 h post transfection and the cover-slips were gently washed with 1 ml $PBS^{+/+}$. Then, 0.5 ml 4 % PFA was added to the cover-slip for the fixation of the cells. After an incubation time of 20 min, PFA was removed and the cover-slips were again gently washed by using 1 ml $PBS^{+/+}$. An amount of 1 ml Triton X-100 was added to the cover-slips for 5 min in order to break up the membrane of the cells. Cover-slips were again washed with 1 ml $PBS^{+/+}$ and then blocked with 3 % BSA for 1 h at room temperature while gently shaking the 6-well plates containing the cover-slips. The 3 % BSA was removed and, in the next step, the cover-slips were incubated with the Phalloidin antibody diluted in 1 %

BSA in a concentration of 1:200 for 2 h with a total volume of 300 µl per well and were shaken gently. After the incubation time, the cover-slips were washed with $PBS^{+/+}$ twice for 5 min at room temperature while being shaken gently. The primary and secondary antibodies were each incubated overnight in a total concentration of 0.7 µl in 300 µl 1 % BSA per well. Two $PBS^{+/+}$ washing steps in between, each for 5 min were carried out while gently shaking the 6-well plates. All antibodies were kept out of direct light by covering the samples with aluminium foil as a protection against paling. Finally, the cover-slips were fixed upside-down on an object glass using a drop of mounting solution also containing DAPI to stain the nucleus of the cell. The slides prepared were kept for 12 h at room temperature following storage for 12 h at 4°C.

4.8 Fluorescence microscopy

The fluorescence microscopy (Nikon TE2000 fluorescence microscope, Nikon Instruments Europe BV, Amsterdam, The Netherlands) was used to verify the transfection efficiency of cells using a fluorescence signal. It is based on the idea of animation of fluorophore-labelled cells or cell compartments by emitted light of specific wavelengths. The light passes through a specific filter to allow the emission of correct wavelengths and is reflected through the objective onto the object; it is also called epifluorescence microscopy. The animated fluorophore of the object then reflects specific wavelengths of light, which are filtered again and detected. The fluorophore labelling is performed by specific antibodies, as described in the immunoblotting section of this thesis. The fixation of the cells is performed as described in the CLSM section. The main differences to CLSM are a lower contrast of the object detected and a fluorophore animation by light and not by laser.

4.9 Statistical methods

The significance of the differences for the parametric data of the MTT assay and FACS analysis, comparing the effects of the C-terminal variants and the GAR domain variants of Ncl, were statistically analysed by comparing the measurements using a one-way analysis of variance (ANOVA) together with a Bonferroni post hoc comparison test regarding the empty vector control (pcDNA3.1flag). Since from literature it is well known that the nucleophosmin

full-length protein overexpression has a dominant-positive effect on cell proliferation, the significance of differences for experiments comparing the Npm full-length protein to the empty vector control were statistically analysed by comparing the measurements using a one-tailed, unpaired t-test (parametric data). The Npm variant (NpmHBD-RNABD) was compared to the empty vector control using a one-tailed, unpaired t-test as well, since the hypothesis of this thesis was, that Npm and Ncl variants do have dominant-negative effects on cells after overexpression (parametric data). The same was done for the Caspase 3 assay. The significance of differences was analysed using *GraphPad Prism 5* (GraphPad Software Inc. Version 5.04). The differences were considered significant at *: $p < 0.05$ (significant); **: $p < 0.01$ (significant); ***: $p < 0.001$ (significant).

5 Results

5.1 Generation of genetically engineered Npm and Ncl variants

The first step was the cloning of different nucleolin (Ncl) and nucleophosmin (Npm) variants. Forward and reverse primers for the respective variants were designed, including a *Bam HI* and *Not I* restriction site. Ncl and Npm variants were amplified from a DNA template using the PCR. The PCR reaction products (5 µl) were analysed on a 1 % analytical agarose gel, which shows 8 Ncl and 4 Npm variants with the correct bp length (Figure 2). The remaining 95 µl of the PCR reaction were separated in a 1 % preparative agarose gel. The respective DNA bands, corresponding to those in Figure 2, were cut out of the gel, according to the protocol of the *Qiagen Gel Extraction Kit*.

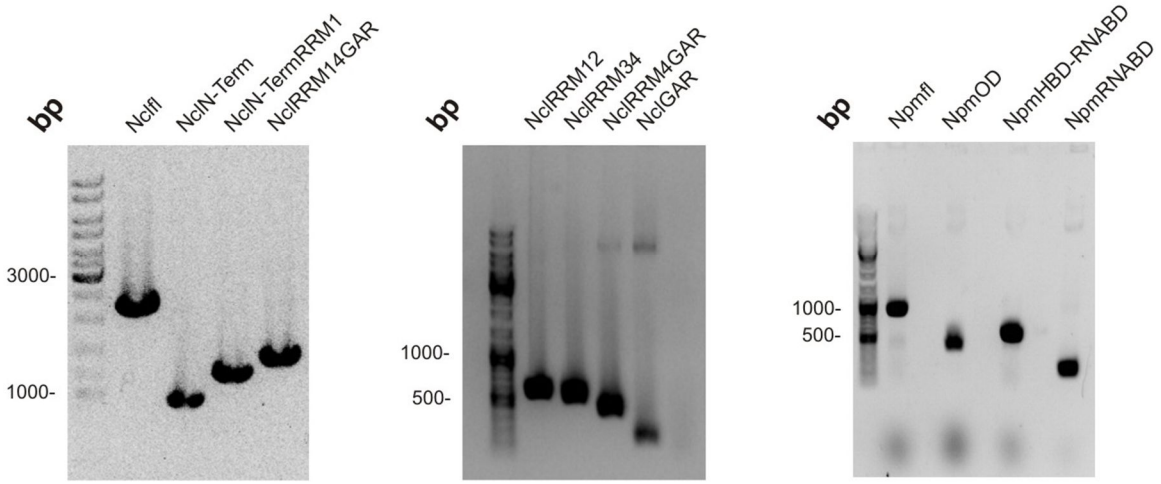

Figure 2: PCR of Ncl and Nmp variants. The PCR results for the Ncl and Npm variants defined, including the full-length proteins. An amount of 5 µl of the PCR reactions were loaded onto a 1% agarose gel. The variants correspond to their specific molecular size in base pairs (bps), visualized by the DNA ladder.

Prepared PCR products and the pcDNA3.1flag vector were digested, by using the *Bam HI* and *Not I* restriction enzymes, ligated and transformed into *E. coli XL1 blue* electro-competent bacteria. The bacteria were cultivated in an overnight culture (12 h) on a 10 cm LB agar plate, containing ampicillin. The transformants obtained were cultured in a 5 ml LB media containing 5 µl of ampicillin for 12 h. The plasmid DNA was prepared according to the protocol of the *Qiagen Mini-Prep Kit*. The plasmids were sent for sequencing in order to determine and verify those clones which contain the Ncl and Npm variants, respectively. The

Ncl and Npm plasmids obtained are shown on an analytical 1 % agarose (Figure 3). For receiving more material, these clones were cultured in 100 ml of LB media containing 100 µl of ampicillin and the respective plasmids. Furthermore, they were prepared according to the protocol of the *NucleoBond Xtra Midi/Maxi Kit*. These plasmids have been used for eukaryotic transfection experiments.

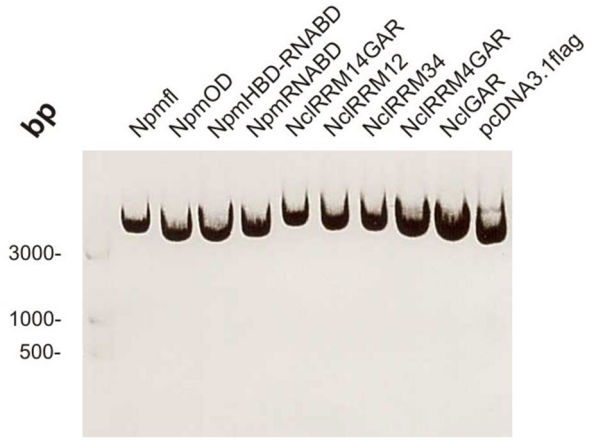

Figure 3: The pcDNA3.1flag plasmid containing various Ncl and Npm variants. All generated and prepared plasmids were loaded on a 1 % agarose gel. The domains are ligated into the pcDNA3.1flag vector corresponding to their specific molecular size in bp, visualized by the DNA ladder shown on the left side. The NpmRNABD domain is larger compared to the calculated molecular size expected.

5.2 Transfection of cells

The concentration and the purity of the plasmid DNA was measured for the transfection of cells by using the *Thermo Scientific nanodrop*. The absorbance at A260/280 was, on average, 1.8, which is acceptable for pure plasmid DNA. The plasmids of the nucleolin and nucleophosmin variants obtained were transfected into mammalian HeLa and Cos-7 cells. Immunoblot experiments of cell lysates at different time points showed a high expression of the variants after 48 h (Figure 4). Therefore, the expression time after transfection for the analysis of all experiments was 48 h.

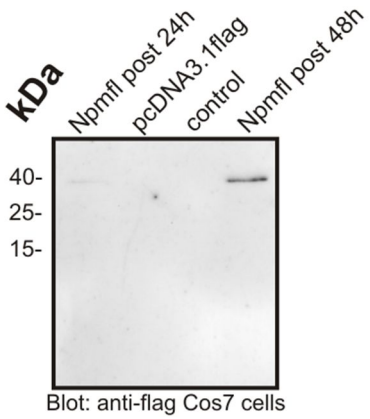

Figure 4: Immunoblot example of Npm variant in Cos-7 cells. The expression for the Npmfl variant is higher after 48 h compared to 24 h. kDa: Kilo-Dalton; pcDNA3.1flag: empty vector control; control: Cos-7 cells only treated with transfection reagent Turbofect.

Transfected HeLa cells were stained with DAPI and anti-flag antibody to verify the efficiency of the transfection method at 48 h. Three different spots at a 20-fold magnification were observed using fluorescence microscopy and the relation between only DAPI-positive and flag-positive cells was evaluated for each transfected nucleolin and nucleophosmin variant (Figure 5).

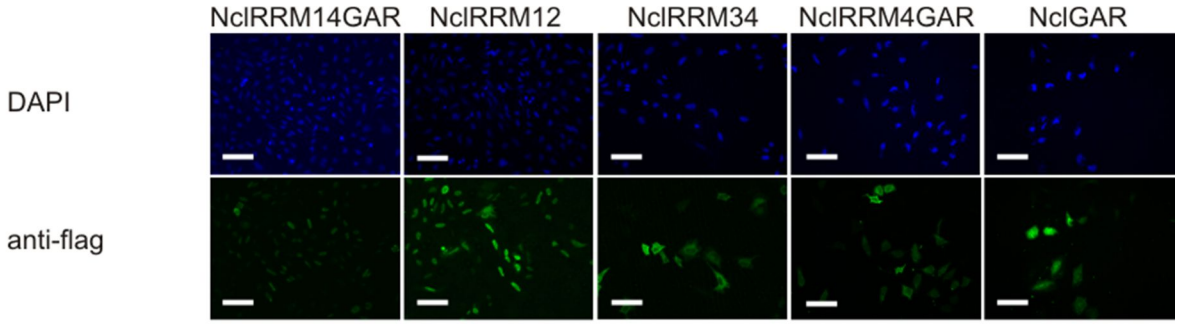

Figure 5: Example of the transfection efficiency in HeLa cells. HeLa cells 48 h post transfection. DAPI and anti-flag stained nucleolin variants at a 20-fold magnification under a fluorescence microscope. The white bar indicates 100 µm; DAPI: 4′,6-Diamidin-2-phenylindol (stained nucleus of HeLa cells); anti-flag: stained nucleolin variants in HeLa cells containing the flag-tag. Scale: 100 µm.

This was carried out twice in two independent experiments and two independent time points. Table 1 in the appendix of this thesis summarises the percentages of the expression of the nucleolin and nucleophosmin variants in transfected cells compared to non-transfected cells. The control experiment was a transfection of the empty pcDNA3.1 flag vector, which showed

no signal when using the anti-flag antibody (compare Figure 19). The transfection efficiency for the nucleolin and nucleophosmin variants was between 33.0 and 49.1 % (Table 1, page 74). It was not possible to detect any signal for the NpmRNABD variant of nucleophosmin (compare Figure 20). To give an example of the morphological appearance of Cos-7 and HeLa cells in bright-field 48 h post transfection with Ncl and Npm variants, compare Figures 6 and 7. The density of the cells was reduced in the transfected cells of Ncl and Npm variants compared to, for example, the mock and the Npmfl variant.

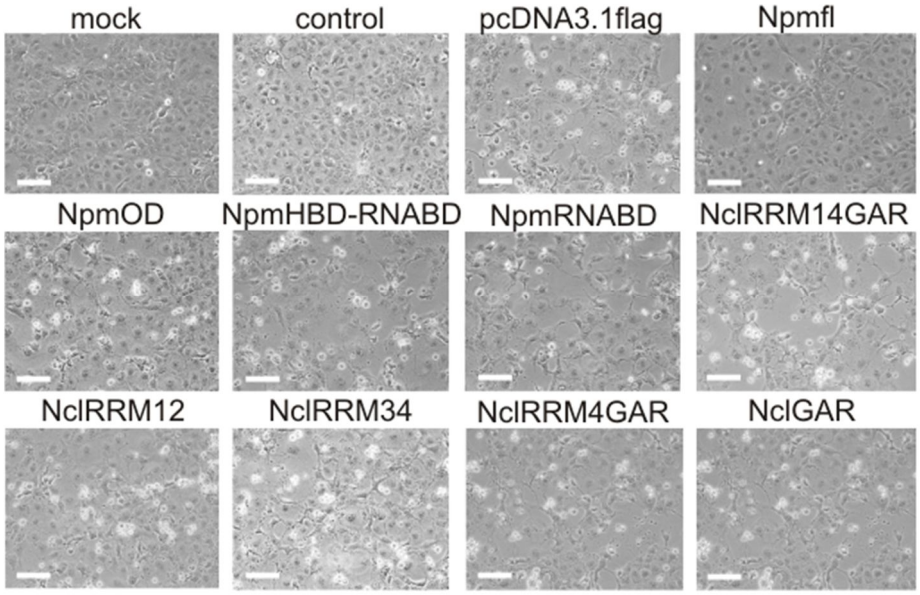

Figure 6: Example of Cos-7 cells' bright-field. Overexpression of Ncl and Npm variants in Cos-7 cells 48 h post transfection. Cells were observed at 20-fold magnification under a fluorescence microscope in bright-field. pcDNA3.1flag: empty vector control; control: Cos-7 cells only treated with transfection reagent Turbofect; mock: untreated Cos-7 cells. Scale: 100 µm.

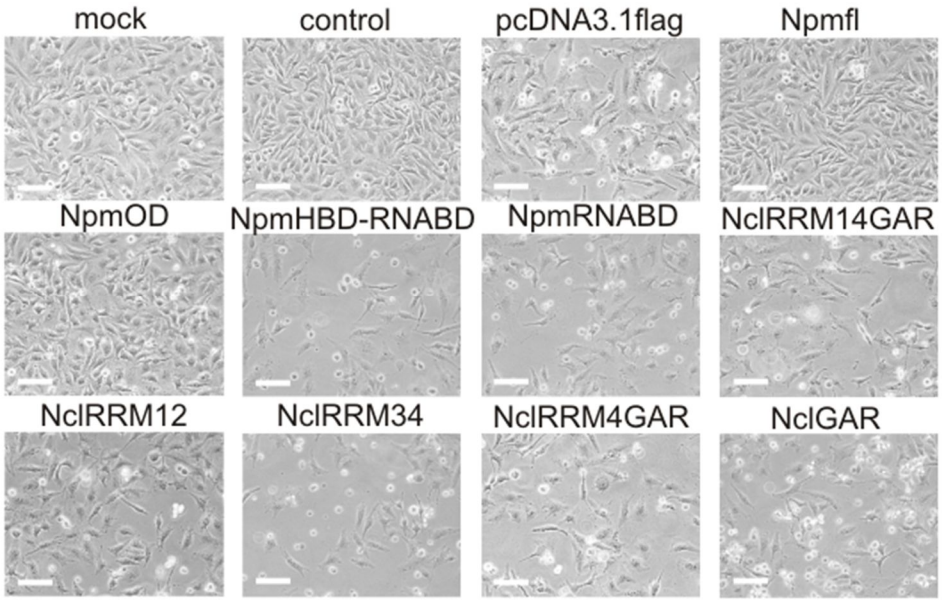

Figure 7: Example of HeLa cells' bright-field. Overexpression of Ncl and Npm variants in HeLa cells 48 h post transfection. Cells were observed at 20-fold magnification under a fluorescence microscope in bright-field. pcDNA3.1flag: empty vector control; control: HeLa cells only treated with transfection reagent Turbofect; mock: untreated HeLa cells. Scale: 100 µm.

5.3 Immunoblot analysis

After microscopic visualization, the expression of the Ncl and Npm variants was the next step verified at the protein level via immunoblotting. Transfected HeLa cells on 10 cm dishes were lysed 48 h post transfection using 250 µl *fish buffer* and the protein concentration of the supernatant after centrifugation was measured using the Bradford Assay. The samples for HeLa cells were diluted with ddH_2O and 5x Laemmli buffer to a total 90 µl sample containing 1.3 µg/µl protein. An amount of 10 µl sample of each nucleolin and nucleophosmin variant was loaded onto an SDS-PAGE and visualized on the immunoblot membrane by using primary and secondary antibodies against the flag-tagged variants, the endogenous nucleolin and nucleophosmin in a dilution of 1/2000 (4 ml milk and 2 µl antibody). The dilution for the primary antibody for α-tubulin was 1/2000 and 1/5000 (10 ml milk and 2 µl antibody) for the secondary antibody. The variants NpmOD, NpmRNABD and NclGAR could not be visualized in HeLa cells by using the immunoblot method. The NclRRM12 showed only a very low expression. The other variants showed a very similar expression in the intensity of their bands compared to the endogenous nucleolin and nucleophosmin full-length proteins which were visualized from the same membrane, but

incubated with the antibody for the endogenous nucleolin and nucleophosmin protein (Figure 8, far right lane). The endogenous α-tubulin protein was visualized on the same membrane to verify the same amount of loading for each variant and to allow a comparison of the expression level of different variants (Figure 8).

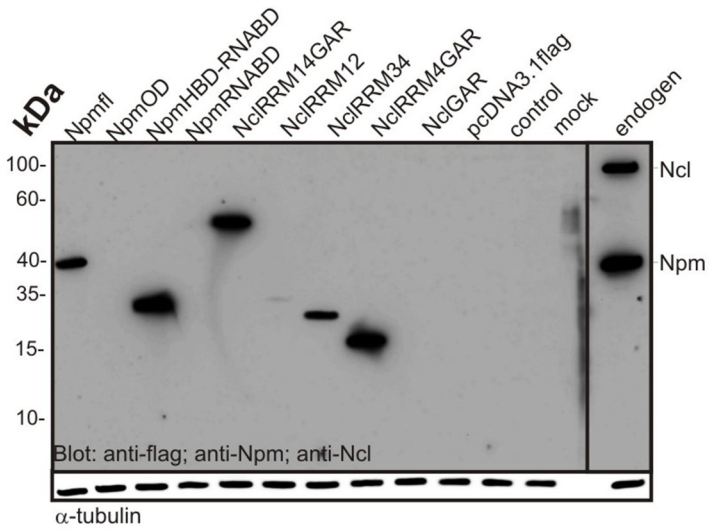

Figure 8: Immunoblot of HeLa cells. Overexpression of Ncl and Npm variants in HeLa cells. Immunoblot of nucleolin and nucleophosmin variants 48 h post transfection in HeLa cells was investigated. The variants are visualized by using the anti-flag antibody. The far right lane shows the expression of endogenous nucleolin and nucleophosmin in HeLa cells by using the specific antibodies. The lower panel shows the endogenous α-tubulin expression as a loading. The variants NpmOD, NpmRNABD and NclGAR could not be visualized in HeLa cells. The variant NclRRM12 only showed a very low expression. kDa: Kilo-Dalton; pcDNA3.1flag: empty vector control; control: HeLa cells only treated with transfection reagent Turbofect; mock: untreated HeLa cells.

Since HeLa cells are human tumour cells, we additionally visualized nucleolin and nucleophosmin variants in a second cell line, the monkey kidney derived Cos-7 cells. Here, the same procedure was carried out as mentioned above for the HeLa cells. The first attempt showed that the variants NpmOD, NpmRNABD and NclGAR, similar to the results in HeLa cells, were not expressed (Figure 9). The variants Npmfl and NclRRM34 only showed a very low expression, which was different from the expression in the HeLa cells. The endogenous α-tubulin loading control expression showed a very weak band for the variant NclGAR. NclGAR was visualized here on a different membrane and added to the figure (Figure 9, far right lane).

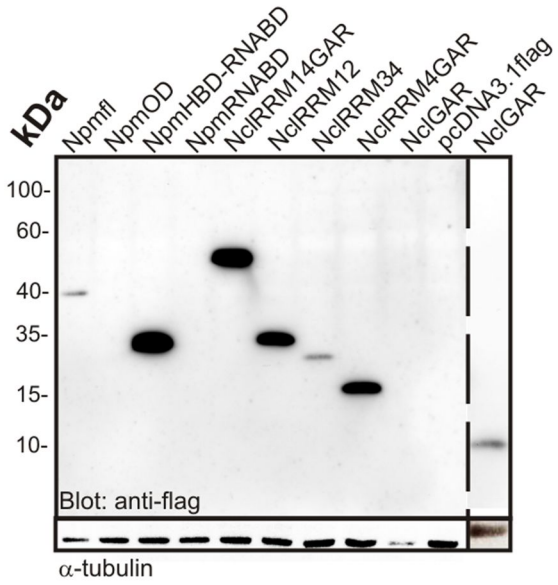

Figure 9: Immunoblot Cos-7 cells first attempt. Overexpression of Ncl and Npm variants in Cos-7 cell. Immunobloting of nucleolin and nucleophosmin variants 48 h post transfection in Cos-7 cells was performed in a first attempt. The variants were visualized by using the anti-flag antibody. The lower panel shows the endogenous α-tubulin expression as a loading control. The variants NpmOD, NpmRNABD and NclGAR could not be visualized. The variants Npmfl and NclRRM34 only showed a very low expression. The loading control for the NclGAR variant only showed a very low intense α-tubulin band. Ncl GAR was expressed on a different membrane (full figure in the appendix of this thesis) and added to the figure (far right lane, broken line). kDa: Kilo-Dalton; pcDNA3.1flag: empty vector control.

The second attempt at trying to visualize the nucleolin and nucleophosmin variants on a protein level in Cos-7 cells by using the immunoblot method showed missing bands for the variants NpmRNABD and NclGAR together with a very weak expression of the variant NclRRM4GAR. This time it was possible to visualize the variant NpmOD at a size of 130 kDa instead of the 13 kDa expected theoretically. This was the first and only time this domain of the nucleophosmin protein was detected by using the immunoblot method. Furthermore, the variant Npmfl showed a very weak band at 40 kDa and an unexpected stronger band at slightly above 130 kDa (Figure 10).

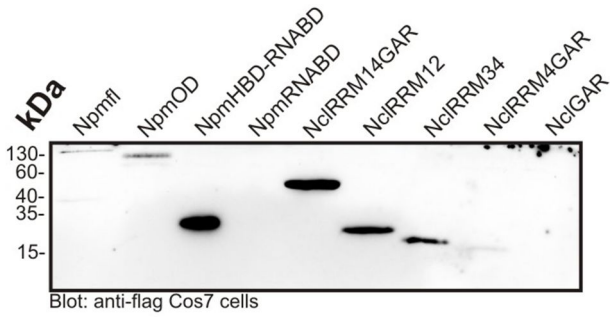

Figure 10: Immunoblot Cos-7 cells second attempt. Immunoblot of Ncl and Npm variants 48 h post transfection in Cos-7 cells. The variants are visualized by using the anti-flag antibody. This time the variants NpmRNABD and NclGAR are not being expressed. NclRRM4GAR only shows a very weak signal. This was the first time the variant NpmOD could be visualized at a size of 130 kDa as well as Npmfl, evidencing the oligomerization of the protein. Npmfl, furthermore, was visualized by a weak band at 40 kDa. kDa: Kilo-Dalton.

Variants of Ncl and Npm were overexpressed in Cos-7 and HeLa cells to verify the effects on the endogenous Ncl and Npm protein by using the immunoblot method. The endogenous proteins were detected by using the anti-Ncl and anti-Npm antibody. The α-tubulin antibody was used as a control for loading. It was not possible to detect any change in the expression of the endogenous proteins by overexpressing Ncl or Npm variants. The flag-tagged variant Npmfl was also detected by the anti-Npm antibody (Figure 11).

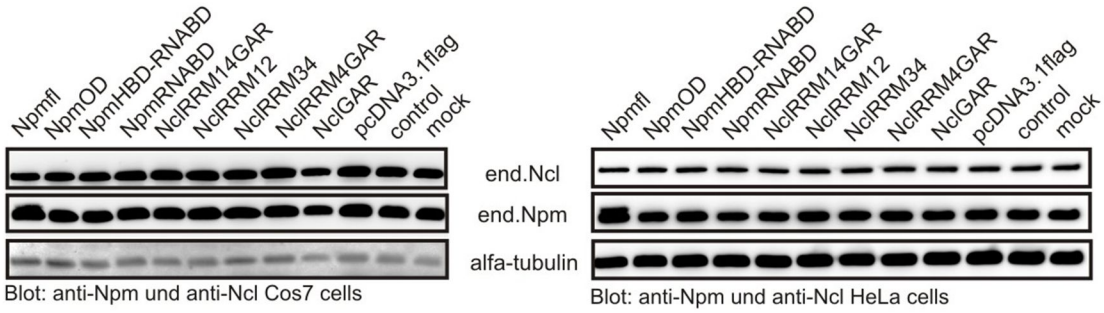

Figure 11: Immunoblot of endogenous proteins in Cos-7 and HeLa cells. Immunoblot of endogenous Ncl and Npm protein expression 48 h upon variant transfection in Cos-7 and HeLa cells. The endogenous proteins are visualized by using the anti-Npm or anti-Ncl antibody. The anti-Npm antibody detects the endogenous Npm protein as well as the flag-tagged full-length Npm protein shown on the far left and middle lane of both images. The α-tubulin antibody was used as a control for loading; pcDNA3.1flag: empty vector control; control: Cos-7 and HeLa cells only treated with transfection reagent Turbofect; mock: untreated Cos-7 and HeLa cells.

5.4 Proliferation assay

After analysing the expression of nucleolin and nucleophosmin variants in HeLa and Cos-7 cells, the next step was to investigate by using the MTT assay whether those overexpressed variants have a dominant-negative effect on the proliferation and viability of the cells mentioned. Variants for this experiment were used in respect of their clear expression visualized in the immunoblot experiments mentioned above. The variants NpmOD and NpmRNABD showed no correct or missing bands in the immunoblot and were, consequently, not included in the following experiments. The variants NclRRM12 and NclGAR only showed sufficient expression in Cos-7 cells in immunoblot analysis. It was not possible to visualize those two variants in immunoblotting in HeLa cells, but it was under the fluorescence microscope and in the confocal laser scanning microscopy (Figures 4 and 19), therefore, they were included in the following experiment to give an impression of their effect on cells. The transfected 96-well plates for each variant were incubated with 40 µl *PromegaCellTiter 96 One Solution Reagent* per well 48 h post transfection. The ongoing bioreduction of this reagent to formazan within the cells was measured by the absorbance at 560 nm and was a direct indicator for the number of living cells, their proliferation and mitochondrial activity. The absorbance for each variant after 60 min in percentage was set in relation to the pcDNA3.1flag empty vector control also transfected. This control was set here to 100 %. HeLa cells reaction (blue bars) to transfected variants was stronger compared to the reaction of Cos-7 cells (red bars). Since it was not possible to visualize the variants NpmOD and NpmRNABD on the immunoblot level correctly, the first experiment (Figure 12) showed the effects of the nucleophosmin full-length and the variant NpmHBD-RNABD compared to the empty vector control in HeLa and Cos-7 cells. Since one of the groups investigated is a full-length protein (Npmfl) and the other is only a part of that protein (NpmHBD-RNABD), those independent groups were statistically compared to the empty vector control (pcDNA3.1flag) by using a one-tailed, unpaired t-test (compare chapter methods: statistical methods). The bar mock represented untreated cells here and was not included in the calculation for the significance of differences. The overexpression of the nucleophosmin full-length protein (Npmfl) had a positive, significant ($p < 0.01$) effect on the viability of HeLa and a significant ($p < 0.001$) effect on Cos-7 cells compared to the empty vector control. The variant NpmHBD-RNABD showed a significant ($p < 0.05$) lower viability in Cos-7 cells and a significant ($p < 0.001$) lower viability in HeLa cells 48 h post transfection.

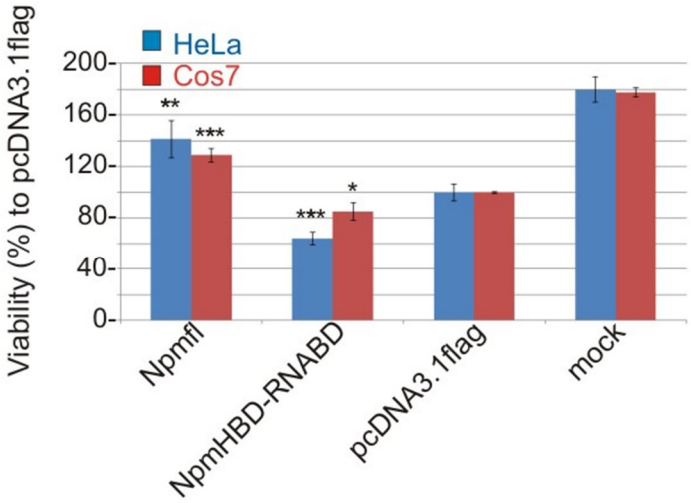

Figure 12: MTT assay of nucleophosmin variants. The graph shows means of percentages of viability in HeLa (blue bars) and Cos-7 cells (red bars) 48 h post transfection compared to the empty vector control (pcDNA3.1flag). The empty vector control was set to 100 %. Bars show means of three different experiments. HeLa: HeLa cells; Cos 7: Cos-7 cells; pcDNA3.1flag: empty vector control; mock: untreated cells; Significance of differences is represented by using a one-tailed, unpaired t-test compared to the empty vector control (pcDNA3.1flag); *: $p < 0.05$ (significant); **: $p < 0.01$ (significant); ***: $p < 0.001$ (significant).

The next step was to investigate the effect of the nucleolin C-terminal variants on the viability of HeLa and Cos-7 cells. Since this experiment included more than one group which needed to be compared to the control, a one-way ANOVA together with a Bonferroni post hoc comparison test was used to compare all the means of the nucleolin variants in a statistical system to the empty vector control (pcDNA3.1flag). The bar mock represented untreated cells here and was not included in the calculation for the significance of differences. All the C-terminal variants of nucleolin showed a significant ($p < 0.001$) decrease on the viability of HeLa and Cos-7 cells, except for the variant NclRRM4GAR in Cos-7 cells, which showed a significant ($p < 0.01$) decrease on the viability and the variants NclRRM12 and NclRRM34 in Cos-7 cells which were not significant (Figure 13).

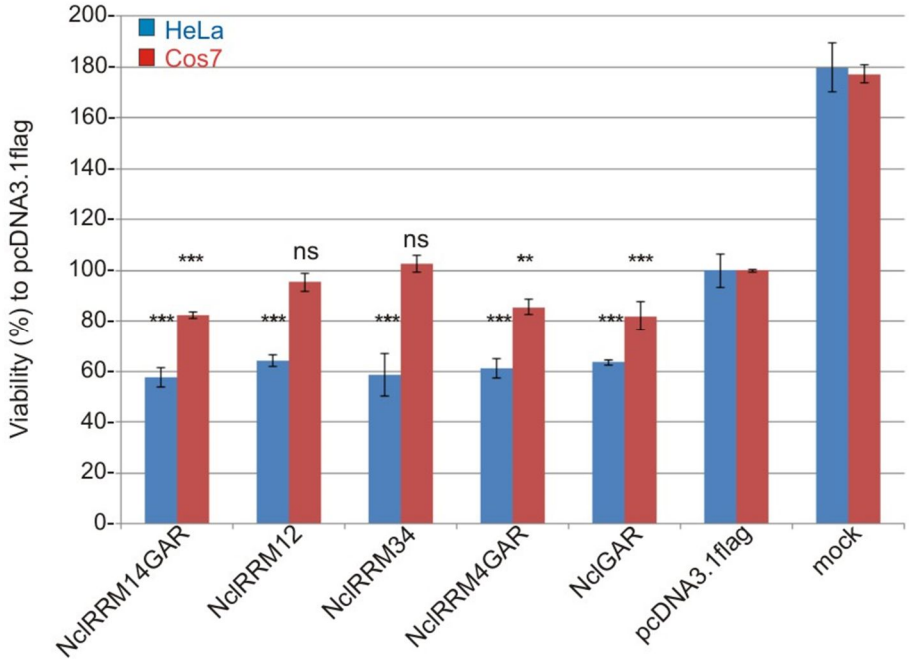

Figure 13: MTT assay of nucleolin C-terminal variants. The graph shows means of percentages of viability in HeLa (blue bars) and Cos-7 cells (red bars) 48 h post transfection compared to the empty vector control (pcDNA3.1flag). The empty vector control was set to 100 %. Bars show means of three different experiments. HeLa: HeLa cells; Cos 7: Cos-7 cells; pcDNA3.1flag: empty vector control; mock: untreated cells. Significance of differences is represented by using a one-way analysis of variance (ANOVA) together with a Bonferroni post hoc comparison test to the empty vector control (pcDNA3.1flag); **: $p < 0.01$ (significant); ***: $p < 0.001$ (significant); ns: not significant.

After analysing the effects of the different nucleolin C-terminal variants on the viability of HeLa and Cos-7 cells, the next step was to repeat the one-way ANOVA with a Bonferroni post hoc comparison test using the same data but this time only those variants including the nucleolin GAR domain compared to the empty vector control (pcDNA3.1flag). The aim here was to shed more light on the proliferation effects of the nucleolin GAR domain connected to the other domains of the nucleolin C-terminus after overexpressing them in HeLa and Cos-7 cells (Figure 14). The bar mock here again represented untreated cells and was not included in the calculation for the significance of differences. All the nucleolin C-terminal variants, including the nucleolin GAR domain, showed a significant ($p < 0.001$) decrease in the viability of HeLa and Cos-7 cells 48 h after overexpression, except for the variants NclRRM14GAR and NclRRM4GAR in Cos-7 cells which had significant effects ($p < 0.01$).

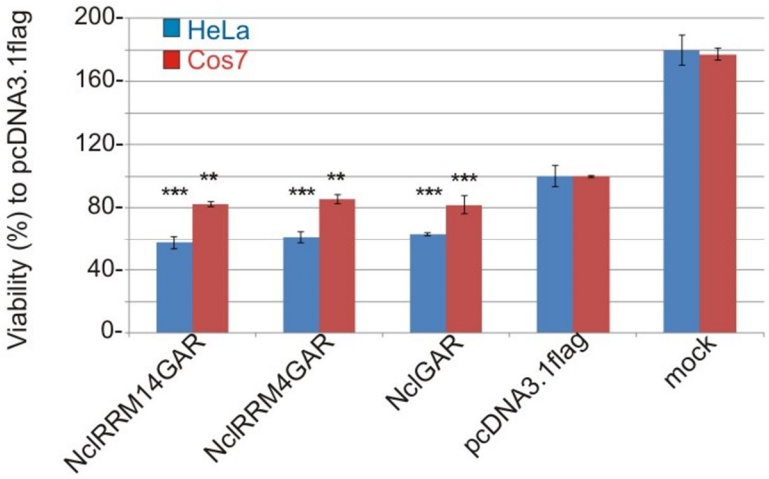

Figure 14: MTT assay of nucleolin variants containing GAR. Graph shows means of percentages of viability in HeLa (blue bars) and Cos-7 cells (red bars) 48 h post transfection compared to the empty vector control (pcDNA3.1flag). The empty vector control was set to 100 %. Bars show means of three different experiments. HeLa: HeLa cells; Cos 7: Cos-7 cells; pcDNA3.1flag: empty vector control; mock: untreated cells. Significance of differences are represented by using a one-way ANOVA together with a Bonferroni post hoc comparison test to the empty vector control (pcDNA3.1flag); **: $p < 0.01$ (significant); ***: $p < 0.001$ (significant).

5.5 FACS analysis

Since the overexpressed nucleolin and nucleophosmin variants disclosed dominant-negative effects on the viability of HeLa and Cos-7 cells using the MTT assay, it was the aim to verify these effects by using another method. The 48 h post transfection cells of transfected 6-well plates (one well for each variant) and their media were collected in a FACS tube. The whole suspension was centrifuged at 1000 rpm at 4 °C for 8 min, the supernatant was discarded and the cells were resuspended again in 1 ml $PBS^{-/-}$. After another centrifuge step, the supernatant was discarded and the cells were resuspended and incubated in 150 µl Nicoletti assay reaction buffer for 2 h. The FACS read-out was then performed by using the BD *CellQuest Pro software*. Here, the amount of Propidium-Iodid attaching to the DNA of the cells was a direct indicator of the amount of DNA within the cells and allowed one to distinguish between different phases of the cell cycle. The graph shows the amount of SubG1 cells in percentage for each variant transfected in HeLa and Cos-7 cells. SubG1 cells represented apoptotic or necrotic cells in this case. The reaction of HeLa cells (blue bars) to transfected variants was stronger compared to the reaction of Cos-7 cells (red bars).

Represented in a similar way to Figure 12, the nucleophosmin full-length protein and the C-terminal variant NpmHBD-RNABD were statistically compared to the empty vector control (pcDNA3.1flag) by using a one-tailed, unpaired t-test. The bar mock here again represented untreated cells and was not included in the calculation for the significance of differences. After overexpression, the nucleophosmin full-length protein (Npmfl) showed a significant ($p < 0.05$) decrease of SubG1 cells in HeLa cells and a significant decrease ($p < 0.01$) in Cos-7 cells compared to the empty vector control. The variant NpmHBD-RNABD showed a significant ($p < 0.01$) increase in the amount of SubG1 cells after overexpression in Cos-7 cells and did not show significant changes in HeLa cells (Figure 15).

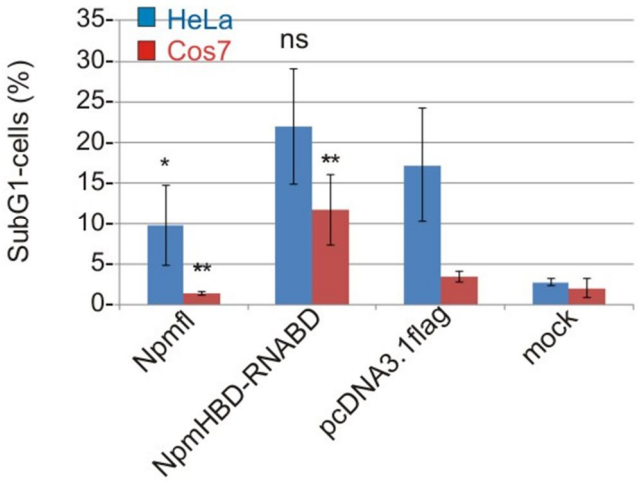

Figure 15: FACS analysis of nucleophosmin variants. The graph shows means of amounts of SubG1 cells in percentages in HeLa (blue bars) and Cos-7 cells (red bars) 48 h post transfection. Bars show means of five different experiments for HeLa cells and four different experiments for Cos-7 cells. HeLa: HeLa cells; Cos 7: Cos-7 cells; pcDNA3.1flag: empty vector control; mock: untreated cells. Significance of differences is represented by using a one-tailed, unpaired t-test compared to the empty vector control (pcDNA3.1flag); *: $p < 0.05$ (significant); **: $p < 0.01$ (significant); ns: not significant.

The next experiment was to compare the variants of the nucleolin C-terminus to the empty vector control. Similar to Figure 13, a one-way ANOVA together with a Bonferroni post hoc comparison test was used to compare all the nucleolin variants in a statistical system to the empty vector control (pcDNA3.1flag). The bar mock represented untreated cells here and was not included in the calculation for the significance of differences. The results in Figure 16 show that none of the nucleolin C-terminal variants have significant effects on the amount of SubG1 cells 48 h post transfection in HeLa and Cos-7 cells, except for the variant NclGAR in

Cos-7 cells, which had a significant ($p < 0.05$) increase compared to the empty vector control (pcDNA3.1flag).

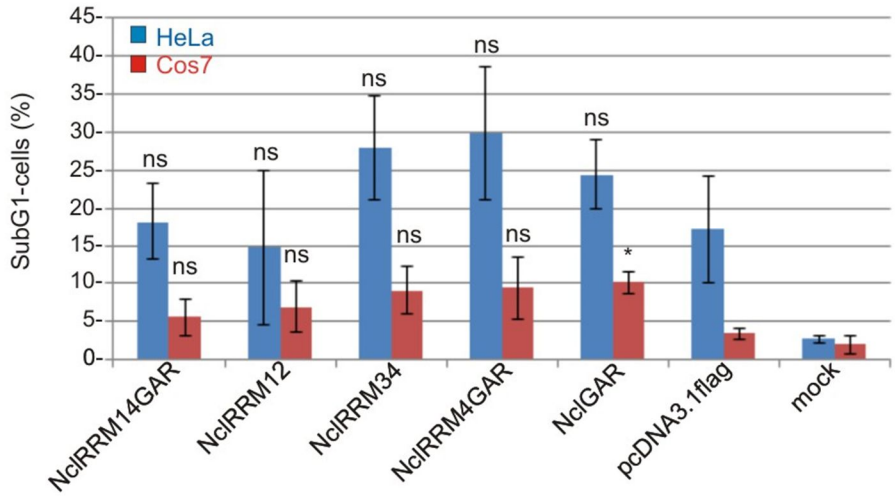

Figure 16: FACS analysis of nucleolin C-terminal variants. The graph shows means of amounts of SubG1 cells in percentages in HeLa (blue bars) and Cos-7 cells (red bars) 48 h post transfection. Bars show means of five different experiments for HeLa cells and four different experiments for Cos-7 cells. HeLa: HeLa cells; Cos 7: Cos-7 cells; pcDNA3.1flag: empty vector control; mock, untreated cells. Significance of differences is represented by using a one-way ANOVA together with a Bonferroni post hoc comparison test to the empty vector control (pcDNA3.1flag); *: $p < 0.05$ (significant); ns: not significant.

In order to investigate the effect of the nucleolin C-terminal variants only containing the GAR domain, similar to Figure 14, a one-way ANOVA together with a Bonferroni post hoc comparison test was repeated, using the same data, to compare those nucleolin variants in a statistical system to the empty vector control (pcDNA3.1flag). The bar mock represented untreated cells here and was not included in the calculation for the significance of differences. In this experiment, the variant NclRRM14GAR showed no significant effects on the amount of SubG1 cells in HeLa or Cos-7 cells. The SubG1 cells were significantly ($p < 0.05$) increased after overexpressing the variant NclRRM4GAR in HeLa and Cos-7 cells. Furthermore, the variant NclGAR showed a significant ($p < 0.05$) increase of the SubG1 cells after overexpressing this domain in Cos-7 cells, but not in HeLa cells (Figure 17).

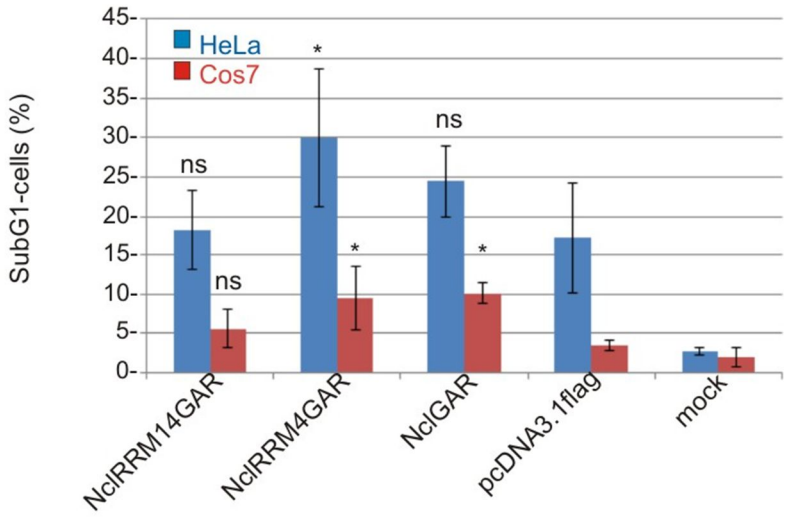

Figure 17: FACS analysis of nucleolin variants containing GAR. The graph shows means of amounts of SubG1 cells in percentages in HeLa (blue bars) and Cos -7 cells (red bars) 48 h post transfection. Bars show means of five different experiments for HeLa cells and four different experiments for Cos-7 cells. HeLa: HeLa cells; Cos 7: Cos-7 cells; pcDNA3.1flag: empty vector control; mock: untreated cells. Significance of differences is represented by using a one-way ANOVA together with a Bonferroni post hoc comparison test to the empty vector control (pcDNA3.1flag); *: $p < 0.05$ (significant); ns: not significant.

5.6 Caspase 3 assay

The caspase 3 assay was performed to verify if the effects measured in the FACS analysis are caused by apoptosis. Therefore, cells and their media transfected on 10 cm dishes were collected in a 50 ml Falcon tube. Further cells were resuspended and washed three times in 1 ml $PBS^{-/-}$ and were then lysated in 100 µl fish buffer. The cleaving of the DEVD substrate was measured as an indicator of the caspase 3 activity. Relative to the DEVD activity in Cos-7 cells, nucleolin and nucleophosmin variants showed no significant differences compared to the pcDNA3.1flag vector control, except for the nucleophosmin full-length protein (Npmfl) compared to the empty vector control (pcDNA3.1flag) by using a one-tailed, unpaired t-test (Figure 18). Using a one-way ANOVA together with a Bonferroni post hoc comparison test to the empty vector control (pcDNA3.1flag), as in the previous experiments, this time showed no significance of differences. HeLa cells only revealed a very low background signal for the DEVD activity (data not shown).

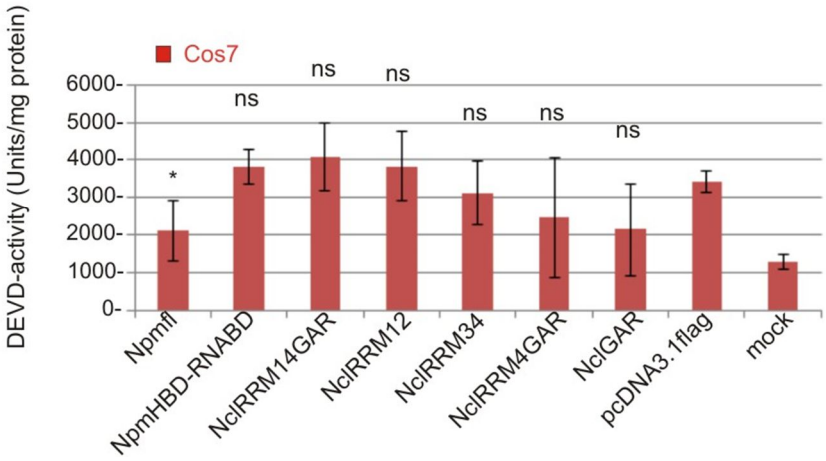

Figure 18: Caspase 3 assay in Cos-7 cells. The graph shows the DEVD activity in units/mg protein as an indicator for the caspase 3 activity 48 h post transfection. Measurements show no significant differences of the nucleolin and nucleophosmin variants in relation to the pcDNA3.1flag empty vector control, except for the nucleophosmin full-length protein (Npmfl). Bars show means of three different experiments. Cos 7: Cos-7 cells; pcDNA3.1flag: empty vector control; mock: untreated cells: Significance of differences is represented by using a one-tailed, unpaired t-test compared to the empty vector control (pcDNA3.1flag); *: $p < 0.05$ (significant); ns: not significant.

5.7 Confocal laser scanning microscopy

The CLSM in HeLa cells was performed to visualize the different nucleolin and nucleophosmin variants in the cells and to find out whether their localization varies from the full-length protein or not. The anti-flag antibody was used to visualize the flag-tagged variants and was incubated overnight in a concentration of 0.7 µl of antibody with 300 µl 1 % BSA per well and cover-slip. The first experiment aimed to study the localization of the nucleolin variants in HeLa cells. The control transfection with the empty vector (pcDNA3.1flag) showed no signal by using the anti-flag antibody. The endogenous nucleolin here was localized to the nucleus and nucleolus of HeLa cells. The variant NclRRM14GAR was located in the nucleus and the nucleolus and shows no differences compared to the endogenous nucleolin protein. The variant NclRRM12 was located in the nucleus, but not in the nucleolus, a main difference compared to the endogenous nucleolin. The localization of the variant NclRRM34 was very different from these two previous findings, as it was found all over the cytoplasm with a more intensive accumulation towards the nucleus, but no or an only very low signal in the nucleus and a missing localization in the nucleolus. The variants

NclRRM4GAR and NclGAR showed a cytoplasmatic localization with no or only very low accumulation in the nucleus and none in the nucleolus. In total, the overexpression of the variants mentioned above had no effect on the localization of the endogenous nucleolin protein, which was usually found in the nucleus and nucleolus (Figure 19).

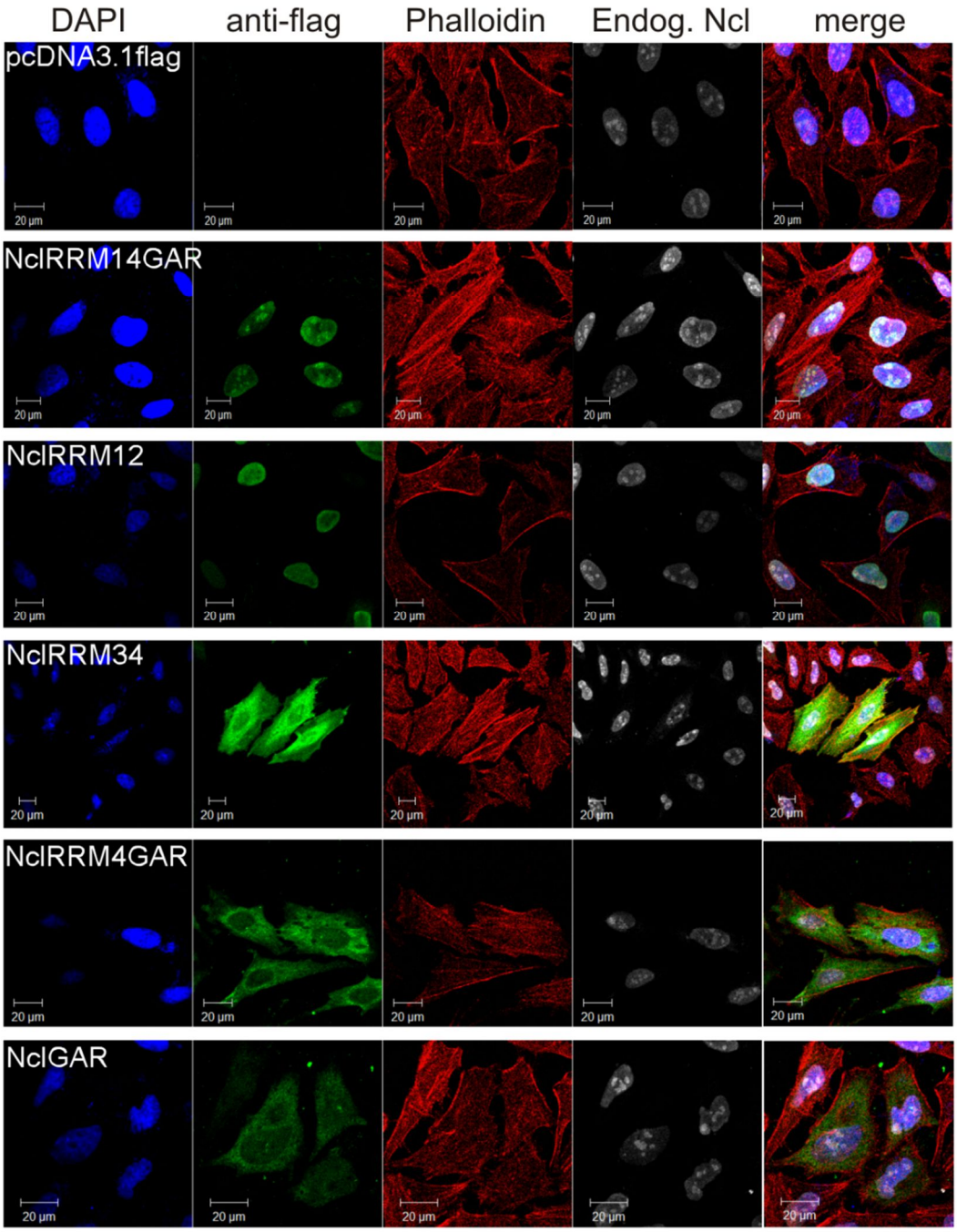

Figure 19: Confocal laser scanning microscopy (CLSM) of nucleolin variants. The images show variants of the nucleolin C-terminus 48 h post transfection in HeLa cells. DAPI: 4′,6-Diamidin-2-phenylindol (stained nucleus of HeLa cells); anti-flag: stained nucleolin variants in HeLa cells containing the flag-tag; Phalloidin:

stained cytoskeleton of HeLa cells; Endog.-Ncl: endogene nucleolin in HeLa cells visualized by using the nucleolin antibody; merge: showing all four signals visualized superimposed over each other. Scale: 20 µm.

The second experiment was to visualize the nucleophosmin variants in HeLa cells. The variant Npmfl, which included the nucleophosmin full-length protein, was located in the nucleolus and also, with a less intense signal, in the nucleoplasm of HeLa cells. The variant NpmOD disclosed localization all over the nucleoplasm and the nucleolus. The signal coming from the nucleoplasm was here more intensive compared to the nucleophosmin full-length protein. The NpmHBD-RNABD domain was located at the edge of the nucleus, but not in the nucleolus. It was not possible to detect any signal for the variant NpmRNABD (Figure 20).

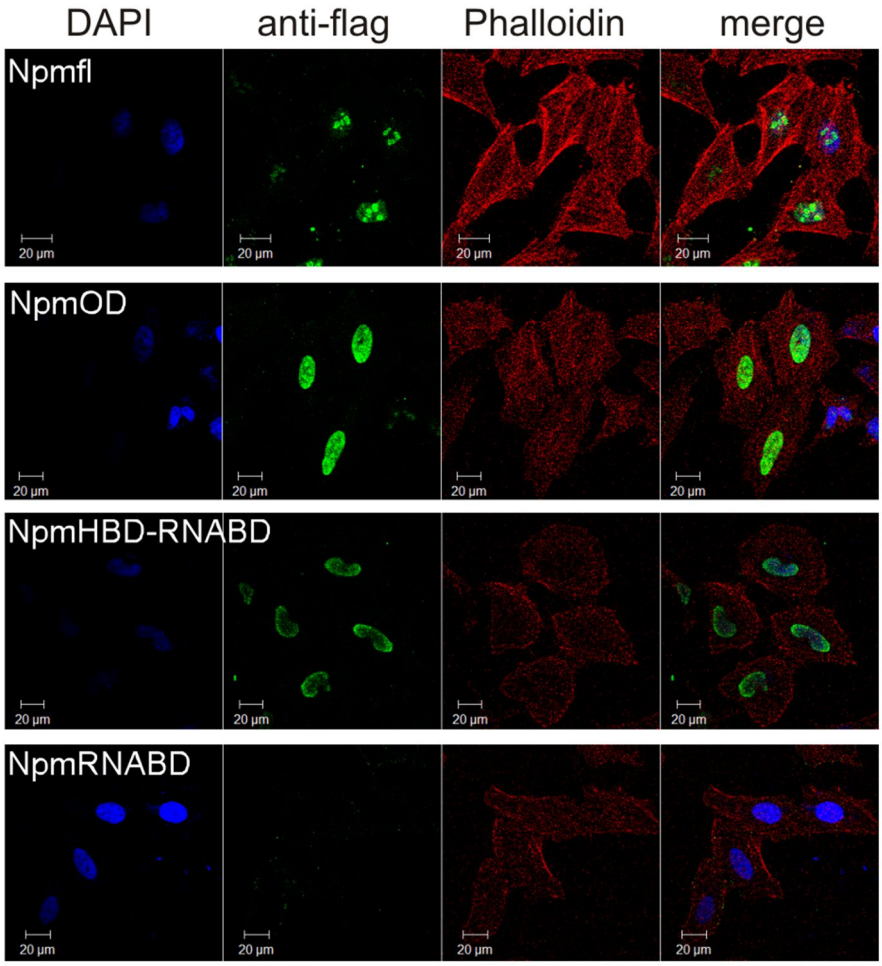

Figure 20: CLSM of nucleophosmin variants. The images show variants of nucleophosmin 48 h post transfection in HeLa cells. DAPI: 4′,6-Diamidin-2-phenylindol (stained nucleus of HeLa cells); anti-flag: stained nucleophosmin variants in HeLa cells containing the flag-tag; Phalloidin: stained cytoskeleton of HeLa cells; merge: showing three signals visualized superimposed over each other. Scale: 20 µm.

6 Discussion

In this study, variants of nucleolin (Ncl) and nucleophosmin (Npm) were transfected in Cos-7 and HeLa cells to gain insights into their potential dominant-negative effects on proliferation. The idea was to interfere with the function of the endogenous full-length proteins by overexpressing individual domains or a combination of them. Amplification and cloning of Ncl and Npm variants out of the respective DNA templates was successful, except for Nclfl, NclN-Term and NclN-TermRRM1 domains. The reason could be the Ncl template with a different N-terminus.

6.1 Immunoblot analysis of the Ncl and Npm variants

Immunoblot analysis showed that nearly all variants were expressed and synthesized, except for NpmRNABD. An interesting observation was the molecular weight of NpmOD at a size of 130 kDa in the immunoblot analysis of Cos-7 cells (Figure 10), instead of the theoretical molecular weight of 13 kDa. NpmOD is one of the most investigated domains and is responsible for the pentameric formation of Npm (Prinos et al., 2011). It is striking that the band observed in the NpmOD lane is slightly smaller than the overexpressed flag-tagged Nmpfl protein (Figure 10, first lane on the left side). One could argue that the 130-kDa band in the NpmOD lane may represent a complex of overexpressed NpmOD with the endogenous Npmfl protein. as previously suggested (Bertwistle et al., 2004), with the difference that this group used a more elongated variant consisting of OD and HBD. NpmRNABD could not be visualized by immunoblotting or by CLSM. Thus, NpmOD and NpmRNABD were not included in the proliferation experiments concerning HeLa and Cos-7 cells.

NclRRM12 and NclGAR showed sufficient expression in Cos-7 cells in the immunoblot analysis. Since they were, however, not sufficiently detected in HeLa cells on an immunoblot level, but were in the CLSM (Figure 19), they were included in the proliferation experiments. Previous studies have reported about difficulties in visualizing a 5-kDa-Myc-tagged GAR domain of nucleolin in the immunoblot (Kim et al., 2005). Therefore, it is very possible that a small sized, flag-tagged NclGAR in this study is expressed in HeLa cells, but can simply not be visualized in immunoblots.

Ncl variants lacking phosphorylation sites have been reported to physically associate with the endogenous Ncl and to interfere with its cellular functions (Xiao et al., 2014). Therefore, we have speculated that overexpressed Ncl and Npm variants may undergo interaction with the endogenous Ncl and Npm in both HeLa and Cos-7 cells, and could then alter their expression pattern, respectively. Data shown in Figure 11 revealed clearly that overexpressed variants of Ncl and Npm affect the amounts of the endogenous Ncl and Npm for 48 h. It can, however, not be excluded that the time point in these experiments was short and a later evaluation after 72 or 96 h may have some effects.

6.2 Npmfl and its effect on cell proliferation

As known from the literature, overexpression of Npmfl has a dominant-positive effect on the proliferation of human leukaemia *HL-60* cells after induction of apoptosis (Hsu and Yung, 2000, Li et al., 2007). Significant effects were found in this study in HeLa and Cos-7 cells overexpressed with Npmfl. Data showed an increased viability in the MTT assay (Figure 12; ~ 35 % in Cos-7 and ~ 40 % in HeLa cells), a decreased amount of SubG1 cells based on the FACS analysis (Figure 15; ~ 2 % in Cos 7 and ~ 7 % in HeLa cells) and a decreased amount of DEVD activity in the caspase 3 assay (Figure 18; ~ 1200 units/mg protein). An empty-vector control (pcDNA3.1flag) was used in these experiments.

6.3 NpmHBD-RNABD and its effect on cell proliferation

The NpmHBD-RNABD variant revealed a significantly dominant-negative effect on the proliferation and viability. Both HeLa (~ 40 %) and Cos 7 (~ 20 %) cells showed a decreased effect using the MTT assay (Figure 12) as well as an increase of SubG1 cells in the FACS analysis (Figure 15; ~ 9 % in Cos-7 and 5 % in HeLa cells) compared to the empty-vector control (pcDNA3.1flag). This effect contradicts the results of a TAT-mediated overexpression of a Npm variant lacking the N-terminus (Zhou et al., 2008). Zhou et al. (2008) reported no significant effects on the proliferation of preleukaemic *stem cells Fancc-/- MEFs* and *WT MEFs* using the MTT assay. The difference here was the TAT-mediated overexpression, which is a little HIV-1-associated domain responsible for transduction (Schwarze et al., 1999)

and the fact that Zhou et al. (2008) used a Npm variant consisting of amino acid 186-294. The NpmHBD-RNABD domain in this study consisted of amino acid 123-294 and included not only the histone-, but also the RNA/DNA-binding domain of Npm. The main functions of Npm are not only the binding to histones, but also the binding to RNA and DNA. It has recently been postulated that the binding to rRNA chromatin by the histone-binding domain depends on the binding of RNA by the RNA- and DNA-binding domain. Additionally, a posttranslational modification, such as phosphorylation, on the IDR of these two domains alters their interaction (Hisaoka et al., 2010, Hisaoka et al., 2014). Thus, the dominant-negative effect of the domains (NpmHBD-RNABD) observed in this study may attributed to their interdependent functions.

Since SubG1 cells in the FACS analysis could represent apoptotic and necrotic cells, the aim of the caspase 3 assay was to shed more light on the effect of the overexpressed Npm variants and to identify apoptotic cells. However, it was not possible to observe a significant increase in the caspase 3 activity as a marker for apoptosis (Figure 18). The reason for this could be the fact that the Cos-7 cells of the variants observed which died from overexpression did not activated the caspase 3 pathway or the assay itself was not sensitive enough. The latter can be underlined by a nearly missing signal for caspase 3 activity in HeLa cells after the overexpression of variants (data not shown). Here another more sensitive method could have been the caspase 3 antibody-referred method using a flow cytometric assay or the TUNEL assay (Zhou et al., 2008). Murano et al. (2008) showed dominant-negative effects of a Npm oligomerization domain on *239Tcells* and *p53-/-MEFs* using a variant consisting of the first 117 amino acids. At the same time, Zhou et al. (2008) revealed dominant-negative effects after overexpressing the TAT-mediated first 174 amino acids in *Fancc-/- MEFs* and *WT MEFs*. To the best of our knowledge, this is the first time evidence of proliferation and viability inhibition through the overexpression of a Npm variant consisting of the histone- together with RNA- and DNA-binding domain (amino acid 123-294) has arisen. Thus, we suggest an important interdependent function of the Npm histone- together with the RNA- and DNA-binding domain reached, for example, through *IDRs*, for an efficient cell proliferation.

6.4 The role of NclGAR in cell proliferation

Since the full-length and the N-terminal variants of Ncl could not be cloned, data with the more C-terminal regions of Ncl were obtained, including NclRRM14GAR, NclRRM12, NclRRM34, NclRRM4GAR and NclGAR. The overexpression of these variants in HeLa and Cos-7 cells revealed a significantly dominant-negative effect on cell proliferation using the MTT assay (Figure 13), except for NclRRM12 and NclRRM34 in Cos-7 cells. Our data showed no significant differences between these variants, such that their effect was about 40 % in HeLa cells and 20 % in Cos-7 cells compared to each other and to the empty vector control (pcDNA3.1flag). To verify the results mentioned, variants were additionally overexpressed and analysed by using the FACS method (Figure 16), screening for SubG1 cells as tools to monitor apoptosis or necrosis. These experiments revealed no significant differences, except for NclGAR in Cos-7 cells. The reason here could be that nucleolin RNA-binding domains are, on the one hand, important for rRNA-binding (Serin et al., 1997), interaction with pre-rRNA (Ginisty et al., 2001) or chaperone function connected to rRNA interaction (Allain et al., 2000). On the other hand, RNA-binding domains are redundant in proliferating cells, where even the presence of a single RRM has been shown to be sufficient for proliferation and survival of the cell in *DT40 chicken B lymphocytes* (Storck et al., 2009).

In this study, using a statistical system comparing all these C-terminal domains to the empty-vector control (pcDNA3.1flag) was not sufficient and disclosed no significance of differences. Storck et al. (2009) reported redundant functions of RRM domains by overexpressing stable transfected variants. However, the role of GAR still remained unclear here. In this study, an additional focus was set on the role of GAR in proliferation and in the C-terminus of nucleolin. Three variants, NclRRM14GAR, NclRRM4GAR and NclGAR were used in a statistically system to observe significant effects on the proliferation in HeLa and Cos-7 cells using the MTT assay and FACS analysis. The cell viability was reduced up to 40 % in HeLa and 20 % in Cos-7 cells (Figure 14). In agreement with these findings, the FACS analysis revealed a 7 % increase of SubG1 cells in Cos-7 cells together with 13 % in HeLa cells (Figure 17). The caspase 3 assay again showed no significant effects (Figure 18). For MTT and FACS results, NclGAR, if connected to the RRM4 domain, seems to be a potent inhibitor of proliferation. Interestingly, the effects mentioned could not be observed in both cell lines using NclGAR alone or the complete C-terminus (NclRRM14GAR) containing NLS, RRM1, RRM2, RRM3, RRM4 and GAR. The single GAR domain itself here showed equal tendency,

but the effect using RRM4GAR was stronger. RRM4GAR has been reported to be a potent binding partner of the human telomerase reverse transcriptase subunit (hTERT) which is a catalytic subunit of the human telomerase. NclRRM4GAR is critical for the localization of hTERT to the nucleolus in *Huh7 hepatoma-derived cancer cells* (Khurts et al., 2004). As suggested in Khurts et al. (2004), overexpression of NclRRM4GAR physically binds and sequestrates the telomerase to the cytoplasm. This effect is probably provided by the lack of the NLS of the RRM4GAR, which, consequently, localizes to the cytoplasm (Figure 19). Thus, this effect may be an explanation for dominant-negative effects of NclRRM4GAR in HeLa and Cos-7 cells as a consequence of its altered localization and function of telomerase leading to a decrease cell proliferation. This conclusion is supported by recent data on proliferation and differentiation of *rat osteoporosis mesenchymal stem cells* upon TERT transfection (Li et al., 2015), a function that is most probably disturbed by overexpressing RRM4GAR, as shown in this study.

Nucleolins GAR domain is reported to be essential for an interaction with the *human replication protein A* (RPA), leading to its inactivation upon cellular stress (Daniely and Borowiec, 2000, Kim et al., 2005). Further, overexpression of myc-tagged NclGAR led to a G1 cell cycle arrest together with a decrease in S-phase cells in *U2-OS cells* (Kim et al., 2005). Even if Kim et al. (2005) did not use a nucleolin variant consisting of RRM4 and GAR, these findings may explain the dominant-negative effects of the variant RRM4GAR on cell proliferation observed in this study. A reason for this effect may be the interaction of GAR as well as RRM4GAR with RPA by reducing DNA replication and affecting cell viability.

6.5 Subcellular localization of Ncl C-terminal variants

The overexpression of the C-terminal region of Ncl (NclRRM14GAR) was shown to localize to the nucleus and also nucleolus of HeLa cells in a very similar way to the endogenous Ncl (Figure 19). These findings are consistent with the assumption that a nuclear translocation of Ncl is mediated by both its NLS and the properties of the RRM domains or the C-terminal GAR domain in binding to nucleolar molecules, such as rRNA (Schmidt-Zachmann and Nigg, 1993). Interestingly, a chloramphenicol acetyltransferase (CAT)-tagged variant of NclRRM14GAR has been transfected to *L929 mouse cells* and was found to be located at the

nucleolus in 50 % of the cells observed, but in 50 % of cases also at the cytoplasm (Creancier et al., 1993). We conclude that an altered localization of NclRRM14GAR was attributed to a possible sensitive reaction to different phases of the cell cycle leading to an additional cytoplasmatic distribution of the variant.

Interestingly, NclRRM12 was located at the nucleoplasm of HeLa cells with no signals in the cytoplasm and the nucleolus (Figure 19), which is due most probably to the presence of the NLS sequence at the N-terminus of the RRM1 domain and the absence of the GAR domain usually localizing to the nucleolus (Heine et al., 1993, Messmer and Dreyer, 1993).

We showed, however, that NclRRM34 and NclRRM4GAR, both with missing NLS sequence were located at the cytoplasm with no or less signals in the nucleus and no signal in the nucleolus (Figure 19) (Schmidt-Zachmann and Nigg, 1993, Khurts et al., 2004). Interestingly, NclRRM4GAR, containing an N-terminal NLS sequence, relocates to the nucleolus, pointing to the essential combination of an NLS sequence together with one RRM and GAR domain that are responsible for the nucleolar localization. A similar study has revealed a nucleoplasmic localization of a Ncl variant, only consisting of a NLS sequence and the RRM4 domain (Creancier et al., 1993).

In this study, NclGAR, however, was located at the cytoplasm of HeLa cells with less signal coming from the nucleoplasm (Figure 19). These results contradict a previous report that has shown a nucleolar localization of NclGAR when overexpressed in *U2-OS cells* (Kim et al., 2005). The difference here was a GFP-tagged variant, which could have altered the fluorescence signal compared to our study in which a flag-tagged variant was used. Furthermore, Creancier et al. (1993) have reported on a CAT-tagged, NLS-containing GAR domain that was located at the nucleoplasm when overexpressed in *L929 mouse cells*. Thus, the exact localization of this single very C-terminal domain of Ncl appears to be dependent on cell type use and remains to be clarified.

6.6 Subcellular localization of Npm variants

Consistent with several other studies (Spector et al., 1984, Chan et al., 1985, Zhou et al., 2008), we also found Npmfl mainly in the nucleoli of HeLa cells with some weak signal in the nucleoplasm (Figure 20).

NpmOD was localized to the nucleoplasm, with a less intense signal also in the nucleoli (Figure 20). These findings are similar to the results of a flag-tagged NpmOD overexpressed in *293T cells* (Bertwistle et al., 2004). It is known from the literature that a variant consisting of the first 174 amino acids, including OD and HBD, is mainly located at the nucleoplasm in *HEK293 cells* (Zhou et al., 2008).

By contrast, NpmHBD-RNABD, consisting of the histone- and RNA/DNA-binding domain, was located at the nucleus, more precisely at its periphery (Figure 20). Consistent findings were reported in *293T-cells*, even if here the localization was described less precisely (Bertwistle et al., 2004). Another similar study has shown nuclear and some nucleolar localization of this variant (Korgaonkar et al., 2005). An explanation for the more nuclear localization of NpmHBD-RNABD is the lack of the oligomerization domain, which seems essential for a nucleolar localization of the Npm protein.

7 Conclusion

Data obtained in this study underline the critical role of the C-terminal domains of Npm and Ncl regarding cell proliferation. Overexpression of these domains in cells appear to interfere with the cellular functions of the endogenous Npm and Ncl proteins and the effects are dominant-negative (Xiao et al., 2014).

The NpmHBD-RNABD domain most probably reveals dominant-negative effects on Npm functions since it is not only important for the interactions with histones and nucleic acids, but also for intramolecular interactions of the Npm protein (Hisaoka et al., 2010, Hisaoka et al., 2014). It was not possible in this study to create all Npm variants. The complete assignment of NpmHBD-RNABD in terms of cell proliferation in comparison to the full-length protein was only possible by comparing those effects to reported effects known from literature (Murano et al., 2008, Zhou et al., 2008). Accordingly, NpmOD and NpmHBD-RNABD revealed similar effects on the cell proliferation. Such a dominant-negative effect of NpmHBD-RNABD may stem from its subcellular localization, which was different from the full-length protein and may, thus, sequester binding partners of the endogenous Npm protein and, consequently, interfere with its functions including regulation of cell proliferation.

The nucleolin GAR domain is an interesting domain with many different interactions as recently reported. Dominant overexpression models for functional analysis of nucleolin in proliferation upon transient transfection have not been reported before, except for phosphorylation deficient variants of Ncl (Xiao et al., 2014). Storck *et al*. (2009) reported a more redundant function of nucleolins RRM domains, but did not describe the role of GAR in cell proliferation. Localization studies of nucleolin deletion variants, containing GAR, or GAR in combination with at least one RRM, showed that GAR is important for the nucleolar localization of Ncl and most probably also for its function in the nucleolus (Creancier et al., 1993). Creancier *et al.* (1993) did not report effects on cell proliferation after overexpression of GAR or RRM domains. G1 cell cycle arrest was reported after overexpressing GAR (Kim et al., 2005). Our data are in line with these findings and demonstrate that GAR alone or at least overexpressed together with RRM4 affected cell proliferation most probably by interfering with the functions of the endogenous nucleolin protein. Data obtained in this thesis emphasise that GAR domain is an important domain within the C-terminus of Ncl and affects Ncl function more than single RRM domains. Thus, Ncl GAR is a key element in nucleolin,

especially for its localization and involvement in cell proliferation. The GAR domain achieves its effect alone as a single domain or at least in combination with one RRM (such as RRM4) most probably due to its very specific protein-protein interactions (Hovanessian et al., 2000, Khurts et al., 2004, Taha et al., 2014) and maybe also due to the unfolding of RNA secondary structure (Ghisolfi et al., 1992a). For the latter, the binding specificity of the RRM domains are required (Ghisolfi et al., 1992b). After trying to approach tumour cell growth by inhibition of nucleolin or its GAR domain (C-terminal 63 amino acids) *via* small peptides (Krust et al., 2011, Benedetti et al., 2015, Palmieri et al., 2015, Gilles et al., 2016), or inhibition of the RNA binding domains (Palmieri et al., 2015, Soundararajan et al., 2009, Gilles et al., 2016) we can conclude that an alternative, more exact aim would be the inhibition of RRM4GAR.

The transient transfection used in this study was not always intense enough concerning its effects within the cell. Stably transfected subdomains could have shown stronger effects on cell proliferation and probably also on the caspase 3 assay. In this way, further experiments may underline how GAR and RRM4GAR interfere exactly with cell proliferation.

It was speculated that overexpressed variants may alter the expression of endogenous Npm and Ncl proteins as analysed in immunoblots after 48 hours (Figure 11). It is possible that these effects are more sensitive to stably transfected variants and not to transient transfection, such as in this study. Furthermore, 72 or 96 h would have been a better time point for measuring these effects in immunoblots.

One possible mechanism by which variants of both proteins undergo dominant negative effects could be the p53 pathway, as recently reported for Ncl (Xiao et al., 2014) or the ARF pathway for Npm as reported by (Bertwistle et al., 2004).

More work will be needed to understand the involvement of the regulatory mechanism of Ncl and Npm in cell proliferation and their role as possible targets for an antiproliferative tumour therapy.

8 References

AHN, J. Y., LIU, X., CHENG, D., PENG, J., CHAN, P. K., WADE, P. A. & YE, K. 2005. Nucleophosmin/B23, a nuclear PI(3,4,5)P(3) receptor, mediates the antiapoptotic actions of NGF by inhibiting CAD. *Mol Cell,* 18**,** 435-45.

ALLAIN, F. H., BOUVET, P., DIECKMANN, T. & FEIGON, J. 2000. Molecular basis of sequence-specific recognition of pre-ribosomal RNA by nucleolin. *EMBO J,* 19**,** 6870-81.

ANGELOV, D., BONDARENKO, V. A., ALMAGRO, S., MENONI, H., MONGELARD, F., HANS, F., MIETTON, F., STUDITSKY, V. M., HAMICHE, A., DIMITROV, S. & BOUVET, P. 2006. Nucleolin is a histone chaperone with FACT-like activity and assists remodeling of nucleosomes. *EMBO J,* 25**,** 1669-79.

BENEDETTI, E., ANTONOSANTE, A., D'ANGELO, M., CRISTIANO, L., GALZIO, R., DESTOUCHES, D., FLORIO, T. M., DHEZ, A. C., ASTARITA, C., CINQUE, B., FIDOAMORE, A., ROSATI, F., CIFONE, M. G., IPPOLITI, R., GIORDANO, A., COURTY, J. & CIMINI, A. 2015. Nucleolin antagonist triggers autophagic cell death in human glioblastoma primary cells and decreased in vivo tumor growth in orthotopic brain tumor model. *Oncotarget,* 6**,** 42091-104.

BERTWISTLE, D., SUGIMOTO, M. & SHERR, C. J. 2004. Physical and functional interactions of the Arf tumor suppressor protein with nucleophosmin/B23. *Mol Cell Biol,* 24**,** 985-96.

BHAT, U. G., JAGADEESWARAN, R., HALASI, M. & GARTEL, A. L. 2011. Nucleophosmin interacts with FOXM1 and modulates the level and localization of FOXM1 in human cancer cells. *J Biol Chem,* 286**,** 41425-33.

BHATT, P., D'AVOUT, C., KANE, N. S., BOROWIEC, J. A. & SAXENA, A. 2012. Specific domains of nucleolin interact with Hdm2 and antagonize Hdm2-mediated p53 ubiquitination. *FEBS J,* 279**,** 370-83.

BIGGIOGERA, M., FAKAN, S., KAUFMANN, S. H., BLACK, A., SHAPER, J. H. & BUSCH, H. 1989. Simultaneous immunoelectron microscopic visualization of protein B23 and C23 distribution in the HeLa cell nucleolus. *J Histochem Cytochem,* 37**,** 1371-4.

BISCHOF, D., PULFORD, K., MASON, D. Y. & MORRIS, S. W. 1997. Role of the nucleophosmin (NPM) portion of the non-Hodgkin's lymphoma-associated NPM-anaplastic lymphoma kinase fusion protein in oncogenesis. *Mol Cell Biol,* 17**,** 2312-25.

BORER, R. A., LEHNER, C. F., EPPENBERGER, H. M. & NIGG, E. A. 1989. Major nucleolar proteins shuttle between nucleus and cytoplasm. *Cell,* 56**,** 379-90.

BOURBON, H. M., PRUDHOMME, M. & AMALRIC, F. 1988. Sequence and structure of the nucleolin promoter in rodents: characterization of a strikingly conserved CpG island. *Gene,* 68**,** 73-84.

BOUVET, P., DIAZ, J. J., KINDBEITER, K., MADJAR, J. J. & AMALRIC, F. 1998. Nucleolin interacts with several ribosomal proteins through its RGG domain. *J Biol Chem,* 273**,** 19025-9.

BUGLER, B., CAIZERGUES-FERRER, M., BOUCHE, G., BOURBON, H. & AMALRIC, F. 1982. Detection and localization of a class of proteins immunologically related to a 100-kDa nucleolar protein. *Eur J Biochem,* 128**,** 475-80.

CAIZERGUES-FERRER, M., BELENGUER, P., LAPEYRE, B., AMALRIC, F., WALLACE, M. O. & OLSON, M. O. 1987. Phosphorylation of nucleolin by a nucleolar type NII protein kinase. *Biochemistry,* 26**,** 7876-83.

CHAN, P. K., ALDRICH, M. & BUSCH, H. 1985. Alterations in immunolocalization of the phosphoprotein B23 in HeLa cells during serum starvation. *Exp Cell Res,* 161**,** 101-10.

CHAN, P. K., CHAN, F. Y., MORRIS, S. W. & XIE, Z. 1997. Isolation and characterization of the human nucleophosmin/B23 (NPM) gene: identification of the YY1 binding site at the 5' enhancer region. *Nucleic Acids Res,* 25**,** 1225-32.

CHAN, W. Y., LIU, Q. R., BORJIGIN, J., BUSCH, H., RENNERT, O. M., TEASE, L. A. & CHAN, P. K. 1989. Characterization of the cDNA encoding human nucleophosmin and studies of its role in normal and abnormal growth. *Biochemistry,* 28**,** 1033-9.

CHANG, J. H. & OLSON, M. O. 1990. Structure of the gene for rat nucleolar protein B23. *J Biol Chem,* 265**,** 18227-33.

CHEN, J., SUN, J., YANG, L., YAN, Y., SHI, W., SHI, J., HUANG, Q. & LAN, Q. 2015. Upregulation of B23 promotes tumor cell proliferation and predicts poor prognosis in glioma. *Biochem Biophys Res Commun,* 466**,** 124-30.

COLOMBO, E., MARINE, J. C., DANOVI, D., FALINI, B. & PELICCI, P. G. 2002. Nucleophosmin regulates the stability and transcriptional activity of p53. *Nat Cell Biol,* 4**,** 529-33.

CREANCIER, L., PRATS, H., ZANIBELLATO, C., AMALRIC, F. & BUGLER, B. 1993. Determination of the functional domains involved in nucleolar targeting of nucleolin. *Mol Biol Cell,* 4**,** 1239-50.

DANIELY, Y. & BOROWIEC, J. A. 2000. Formation of a complex between nucleolin and replication protein A after cell stress prevents initiation of DNA replication. *J Cell Biol,* 149**,** 799-810.

DAS, S., CONG, R., SHANDILYA, J., SENAPATI, P., MOINDROT, B., MONIER, K., DELAGE, H., MONGELARD, F., KUMAR, S., KUNDU, T. K. & BOUVET, P. 2013. Characterization of nucleolin K88 acetylation defines a new pool of nucleolin colocalizing with pre-mRNA splicing factors. *FEBS Lett,* 587**,** 417-24.

DERENZINI, M., PESSION, A. & TRERE, D. 1990. Quantity of nucleolar silver-stained proteins is related to proliferating activity in cancer cells. *Lab Invest,* 63**,** 137-40.

DERGUNOVA, N., BULYCHEVA, T. I., ARTEMENKO, E. G., SHPAKOVA, A. P., PEGOVA, A. N., GEMJIAN, E. G., DUDNIK, O. A., ZATSEPINA, O. V. & MALASHENKO, O. S. 2002. A major nucleolar protein B23 as a marker of proliferation activity of human peripheral lymphocytes. *Immunol Lett,* 83**,** 67-72.

DESTOUCHES, D., EL KHOURY, D., HAMMA-KOURBALI, Y., KRUST, B., ALBANESE, P., KATSORIS, P., GUICHARD, G., BRIAND, J. P., COURTY, J. & HOVANESSIAN, A. G. 2008. Suppression of tumor growth and angiogenesis by a specific antagonist of the cell-surface expressed nucleolin. *PLoS One,* 3**,** e2518.

DHAR, S. K. & ST CLAIR, D. K. 2009. Nucleophosmin blocks mitochondrial localization of p53 and apoptosis. *J Biol Chem,* 284**,** 16409-18.

DUTTA, S., AKEY, I. V., DINGWALL, C., HARTMAN, K. L., LAUE, T., NOLTE, R. T., HEAD, J. F. & AKEY, C. W. 2001. The crystal structure of nucleoplasmin-core: implications for histone binding and nucleosome assembly. *Mol Cell,* 8**,** 841-53.

ERARD, M. S., BELENGUER, P., CAIZERGUES-FERRER, M., PANTALONI, A. & AMALRIC, F. 1988. A major nucleolar protein, nucleolin, induces chromatin decondensation by binding to histone H1. *Eur J Biochem,* 175**,** 525-30.

FALINI, B., BOLLI, N., SHAN, J., MARTELLI, M. P., LISO, A., PUCCIARINI, A., BIGERNA, B., PASQUALUCCI, L., MANNUCCI, R., ROSATI, R., GORELLO, P., DIVERIO, D., ROTI, G., TIACCI, E., CAZZANIGA, G., BIONDI, A., SCHNITTGER, S., HAFERLACH, T., HIDDEMANN, W., MARTELLI, M. F., GU, W., MECUCCI, C. & NICOLETTI, I. 2006. Both carboxy-terminus NES motif and mutated tryptophan(s) are crucial for aberrant nuclear export of nucleophosmin leukemic mutants in NPMc+ AML. *Blood,* 107**,** 4514-23.

FALINI, B., MECUCCI, C., TIACCI, E., ALCALAY, M., ROSATI, R., PASQUALUCCI, L., LA STARZA, R., DIVERIO, D., COLOMBO, E., SANTUCCI, A., BIGERNA, B., PACINI, R., PUCCIARINI, A., LISO, A., VIGNETTI, M., FAZI, P., MEANI, N., PETTIROSSI, V., SAGLIO, G., MANDELLI, F., LO-COCO, F., PELICCI, P. G. & MARTELLI, M. F. 2005. Cytoplasmic nucleophosmin in acute myelogenous leukemia with a normal karyotype. *N Engl J Med,* 352**,** 254-66.

FELGNER, P. L., GADEK, T. R., HOLM, M., ROMAN, R., CHAN, H. W., WENZ, M., NORTHROP, J. P., RINGOLD, G. M. & DANIELSEN, M. 1987. Lipofection: a highly efficient, lipid-mediated DNA-transfection procedure. *Proc Natl Acad Sci U S A,* 84**,** 7413-7.

8 References

FIELDS, A. P., KAUFMANN, S. H. & SHAPER, J. H. 1986. Analysis of the internal nuclear matrix. Oligomers of a 38 kD nucleolar polypeptide stabilized by disulfide bonds. *Exp Cell Res,* 164**,** 139-53.

FU, L. & BENCHIMOL, S. 1997. Participation of the human p53 3'UTR in translational repression and activation following gamma-irradiation. *EMBO J,* 16**,** 4117-25.

FULWYLER, M. J. 1965. Electronic separation of biological cells by volume. *Science,* 150**,** 910-1.

GADAD, S. S., SENAPATI, P., SYED, S. H., RAJAN, R. E., SHANDILYA, J., SWAMINATHAN, V., CHATTERJEE, S., COLOMBO, E., DIMITROV, S., PELICCI, P. G., RANGA, U. & KUNDU, T. K. 2011. The multifunctional protein nucleophosmin (NPM1) is a human linker histone H1 chaperone. *Biochemistry,* 50**,** 2780-9.

GALZIO, R., ROSATI, F., BENEDETTI, E., CRISTIANO, L., ALDI, S., MEI, S., D'ANGELO, B., GENTILE, R., LAURENTI, G., CIFONE, M. G., GIORDANO, A. & CIMINI, A. 2012. Glycosilated nucleolin as marker for human gliomas. *J Cell Biochem,* 113**,** 571-9.

GHISOLFI, L., JOSEPH, G., AMALRIC, F. & ERARD, M. 1992a. The glycine-rich domain of nucleolin has an unusual supersecondary structure responsible for its RNA-helix-destabilizing properties. *J Biol Chem,* 267**,** 2955-9.

GHISOLFI, L., KHARRAT, A., JOSEPH, G., AMALRIC, F. & ERARD, M. 1992b. Concerted activities of the RNA recognition and the glycine-rich C-terminal domains of nucleolin are required for efficient complex formation with pre-ribosomal RNA. *Eur J Biochem,* 209**,** 541-8.

GILLES, M. E., MAIONE, F., COSSUTTA, M., CARPENTIER, G., CARUANA, L., DI MARIA, S., HOUPPE, C., DESTOUCHES, D., SHCHORS, K., PROCHASSON, C., MONGELARD, F., LAMBA, S., BARDELLI, A., BOUVET, P., COUVELARD, A., COURTY, J., GIRAUDO, E. & CASCONE, I. 2016. Nucleolin targeting impairs the progression of pancreatic cancer and promotes the normalization of tumor vasculature. *Cancer Res*.

GINISTY, H., AMALRIC, F. & BOUVET, P. 1998. Nucleolin functions in the first step of ribosomal RNA processing. *EMBO J,* 17**,** 1476-86.

GINISTY, H., AMALRIC, F. & BOUVET, P. 2001. Two different combinations of RNA-binding domains determine the RNA binding specificity of nucleolin. *J Biol Chem,* 276**,** 14338-43.

GRAHAM, F. L. & VAN DER EB, A. J. 1973. A new technique for the assay of infectivity of human adenovirus 5 DNA. *Virology,* 52**,** 456-67.

GRINSTEIN, E., DU, Y., SANTOURLIDIS, S., CHRIST, J., UHRBERG, M. & WERNET, P. 2007. Nucleolin regulates gene expression in CD34-positive hematopoietic cells. *J Biol Chem,* 282**,** 12439-49.

GRUMMITT, C. G., TOWNSLEY, F. M., JOHNSON, C. M., WARREN, A. J. & BYCROFT, M. 2008. Structural consequences of nucleophosmin mutations in acute myeloid leukemia. *J Biol Chem,* 283**,** 23326-32.

GURTU, V., KAIN, S. R. & ZHANG, G. 1997. Fluorometric and colorimetric detection of caspase activity associated with apoptosis. *Anal Biochem,* 251**,** 98-102.

HEINE, M. A., RANKIN, M. L. & DIMARIO, P. J. 1993. The Gly/Arg-rich (GAR) domain of Xenopus nucleolin facilitates in vitro nucleic acid binding and in vivo nucleolar localization. *Mol Biol Cell,* 4**,** 1189-204.

HERRERA, J. E., SAVKUR, R. & OLSON, M. O. 1995. The ribonuclease activity of nucleolar protein B23. *Nucleic Acids Res,* 23**,** 3974-9.

HINGORANI, K., SZEBENI, A. & OLSON, M. O. 2000. Mapping the functional domains of nucleolar protein B23. *J Biol Chem,* 275**,** 24451-7.

HISAOKA, M., NAGATA, K. & OKUWAKI, M. 2014. Intrinsically disordered regions of nucleophosmin/B23 regulate its RNA binding activity through their inter- and intra-molecular association. *Nucleic Acids Res,* 42**,** 1180-95.

HISAOKA, M., UESHIMA, S., MURANO, K., NAGATA, K. & OKUWAKI, M. 2010. Regulation of nucleolar chromatin by B23/nucleophosmin jointly depends upon its RNA binding activity and transcription factor UBF. *Mol Cell Biol,* 30**,** 4952-64.

HOVANESSIAN, A. G., PUVION-DUTILLEUL, F., NISOLE, S., SVAB, J., PERRET, E., DENG, J. S. & KRUST, B. 2000. The cell-surface-expressed nucleolin is associated with the actin cytoskeleton. *Exp Cell Res,* 261**,** 312-28.

HSU, C. Y. & YUNG, B. Y. 2000. Over-expression of nucleophosmin/B23 decreases the susceptibility of human leukemia HL-60 cells to retinoic acid-induced differentiation and apoptosis. *Int J Cancer,* 88**,** 392-400.

ITAHANA, K., BHAT, K. P., JIN, A., ITAHANA, Y., HAWKE, D., KOBAYASHI, R. & ZHANG, Y. 2003. Tumor suppressor ARF degrades B23, a nucleolar protein involved in ribosome biogenesis and cell proliferation. *Mol Cell,* 12**,** 1151-64.

JIAN, Y., GAO, Z., SUN, J., SHEN, Q., FENG, F., JING, Y. & YANG, C. 2009. RNA aptamers interfering with nucleophosmin oligomerization induce apoptosis of cancer cells. *Oncogene,* 28**,** 4201-11.

JIANG, P. S. & YUNG, B. Y. 1999. Down-regulation of nucleophosmin/B23 mRNA delays the entry of cells into mitosis. *Biochem Biophys Res Commun,* 257**,** 865-70.

KHURTS, S., MASUTOMI, K., DELGERMAA, L., ARAI, K., OISHI, N., MIZUNO, H., HAYASHI, N., HAHN, W. C. & MURAKAMI, S. 2004. Nucleolin interacts with telomerase. *J Biol Chem,* 279**,** 51508-15.

KIM, K., DIMITROVA, D. D., CARTA, K. M., SAXENA, A., DARAS, M. & BOROWIEC, J. A. 2005. Novel checkpoint response to genotoxic stress mediated by nucleolin-replication protein a complex formation. *Mol Cell Biol,* 25**,** 2463-74.

KORGAONKAR, C., HAGEN, J., TOMPKINS, V., FRAZIER, A. A., ALLAMARGOT, C., QUELLE, F. W. & QUELLE, D. E. 2005. Nucleophosmin (B23) targets ARF to nucleoli and inhibits its function. *Mol Cell Biol,* 25**,** 1258-71.

KRUST, B., EL KHOURY, D., NONDIER, I., SOUNDARAMOURTY, C. & HOVANESSIAN, A. G. 2011. Targeting surface nucleolin with multivalent HB-19 and related Nucant pseudopeptides results in distinct inhibitory mechanisms depending on the malignant tumor cell type. *BMC Cancer,* 11**,** 333.

KUO, M. L., DEN BESTEN, W., BERTWISTLE, D., ROUSSEL, M. F. & SHERR, C. J. 2004. N-terminal polyubiquitination and degradation of the Arf tumor suppressor. *Genes Dev,* 18**,** 1862-74.

KURKI, S., PELTONEN, K., LATONEN, L., KIVIHARJU, T. M., OJALA, P. M., MEEK, D. & LAIHO, M. 2004. Nucleolar protein NPM interacts with HDM2 and protects tumor suppressor protein p53 from HDM2-mediated degradation. *Cancer Cell,* 5**,** 465-75.

KUSAKAWA, T., SHIMAKAMI, T., KANEKO, S., YOSHIOKA, K. & MURAKAMI, S. 2007. Functional interaction of hepatitis C Virus NS5B with Nucleolin GAR domain. *J Biochem,* 141**,** 917-27.

LAEMMLI, U. K. 1970. Cleavage of structural proteins during the assembly of the head of bacteriophage T4. *Nature,* 227**,** 680-5.

LAMBERT, B. & BUCKLE, M. 2006. Characterisation of the interface between nucleophosmin (NPM) and p53: potential role in p53 stabilisation. *FEBS Lett,* 580**,** 345-50.

LAPEYRE, B., AMALRIC, F., GHAFFARI, S. H., RAO, S. V., DUMBAR, T. S. & OLSON, M. O. 1986. Protein and cDNA sequence of a glycine-rich, dimethylarginine-containing region located near the carboxyl-terminal end of nucleolin (C23 and 100 kDa). *J Biol Chem,* 261**,** 9167-73.

LEE, H., KIM, H., KANG, J., LEE, B., HA, J., YOON, H., LIM, S., JUNG, G. & SUH, S. 2007. Crystal structure of human nucleophosmin-core reveals plasticity of the pentamer-pentamer interface. *Proteins,* 69**,** 672-678.

LEITINGER, N. & WESIERSKA-GADEK, J. 1993. ADP-ribosylation of nucleolar proteins in HeLa tumor cells. *J Cell Biochem,* 52**,** 153-8.

LI, C., WEI, G., GU, Q., WANG, Q., TAO, S. & XU, L. 2015. Proliferation and differentiation of rat osteoporosis mesenchymal stem cells (MSCs) after telomerase reverse transcriptase (TERT) transfection. *Med Sci Monit,* 21**,** 845-54.

LI, J., SEJAS, D. P., BURMA, S., CHEN, D. J. & PANG, Q. 2007. Nucleophosmin suppresses oncogene-induced apoptosis and senescence and enhances oncogenic cooperation in cells with genomic instability. *Carcinogenesis,* 28**,** 1163-70.

LI, J., ZHANG, X., SEJAS, D. P. & PANG, Q. 2005. Negative regulation of p53 by nucleophosmin antagonizes stress-induced apoptosis in human normal and malignant hematopoietic cells. *Leuk Res,* 29**,** 1415-23.

LI, Z. & HANN, S. R. 2013. Nucleophosmin is essential for c-Myc nucleolar localization and c-Myc-mediated rDNA transcription. *Oncogene,* 32**,** 1988-94.

LISCHWE, M. A., SMETANA, K., OLSON, M. O. & BUSCH, H. 1979. Proteins C23 and B23 are the major nucleolar silver staining proteins. *Life Sci,* 25**,** 701-8.

LIU, W. H. & YUNG, B. Y. 1998. Mortalization of human promyelocytic leukemia HL-60 cells to be more susceptible to sodium butyrate-induced apoptosis and inhibition of telomerase activity by down-regulation of nucleophosmin/B23. *Oncogene,* 17**,** 3055-64.

MALKIN, D., LI, F. P., STRONG, L. C., FRAUMENI, J. F., JR., NELSON, C. E., KIM, D. H., KASSEL, J., GRYKA, M. A., BISCHOFF, F. Z., TAINSKY, M. A. & ET AL. 1990. Germ line p53 mutations in a familial syndrome of breast cancer, sarcomas, and other neoplasms. *Science,* 250**,** 1233-8.

MEHES, G. & PAJOR, L. 1995. Nucleolin and fibrillarin expression in stimulated lymphocytes and differentiating HL-60 cells. A flow cytometric assay. *Cell Prolif,* 28**,** 329-36.

MESSMER, B. & DREYER, C. 1993. Requirements for nuclear translocation and nucleolar accumulation of nucleolin of Xenopus laevis. *Eur J Cell Biol,* 61**,** 369-82.

METALLO, S. 2010. Intrinsically disordered proteins are potential drug targets. *Current opinion in chemical biology,* 14**,** 481-488.

MOSMANN, T. 1983. Rapid colorimetric assay for cellular growth and survival: application to proliferation and cytotoxicity assays. *J Immunol Methods,* 65**,** 55-63.

MOURMOURAS, V., CEVENINI, G., COSCI, E., EPISTOLATO, M. C., BIAGIOLI, M., BARBAGLI, L., LUZI, P., MANNUCCI, S. & MIRACCO, C. 2009. Nucleolin protein expression in cutaneous melanocytic lesions. *J Cutan Pathol,* 36**,** 637-46.

MULLIS, K. B. & FALOONA, F. A. 1987. Specific synthesis of DNA in vitro via a polymerase-catalyzed chain reaction. *Methods Enzymol,* 155**,** 335-50.

MURANO, K., OKUWAKI, M., HISAOKA, M. & NAGATA, K. 2008. Transcription regulation of the rRNA gene by a multifunctional nucleolar protein, B23/nucleophosmin, through its histone chaperone activity. *Mol Cell Biol,* 28**,** 3114-26.

NAKAGAWA, M., KAMEOKA, Y. & SUZUKI, R. 2005. Nucleophosmin in acute myelogenous leukemia. *N Engl J Med,* 352**,** 1819-20; author reply 1819-20.

NAMBOODIRI, V. M., AKEY, I. V., SCHMIDT-ZACHMANN, M. S., HEAD, J. F. & AKEY, C. W. 2004. The structure and function of Xenopus NO38-core, a histone chaperone in the nucleolus. *Structure,* 12**,** 2149-60.

NEUMANN, E., SCHAEFER-RIDDER, M., WANG, Y. & HOFSCHNEIDER, P. H. 1982. Gene transfer into mouse lyoma cells by electroporation in high electric fields. *EMBO J,* 1**,** 841-5.

NICOLETTI, I., MIGLIORATI, G., PAGLIACCI, M. C., GRIGNANI, F. & RICCARDI, C. 1991. A rapid and simple method for measuring thymocyte apoptosis by propidium iodide staining and flow cytometry. *J Immunol Methods,* 139**,** 271-9.

NISHIMURA, Y., OHKUBO, T., FURUICHI, Y. & UMEKAWA, H. 2002. Tryptophans 286 and 288 in the C-terminal region of protein B23.1 are important for its nucleolar localization. *Biosci Biotechnol Biochem,* 66**,** 2239-42.

NISOLE, S., SAID, E. A., MISCHE, C., PREVOST, M. C., KRUST, B., BOUVET, P., BIANCO, A., BRIAND, J. P. & HOVANESSIAN, A. G. 2002. The anti-HIV pentameric pseudopeptide HB-19 binds the C-terminal end of nucleolin and prevents anchorage of virus particles in the plasma membrane of target cells. *J Biol Chem,* 277**,** 20877-86.

NOURI, K., MOLL, J. M., MILROY, L. G., HAIN, A., DVORSKY, R., AMIN, E., LENDERS, M., NAGEL-STEGER, L., HOWE, S., SMITS, S. H., HENGEL, H., SCHMITT, L., MUNK, C., BRUNSVELD, L. & AHMADIAN, M. R. 2015. Biophysical Characterization of Nucleophosmin Interactions with Human Immunodeficiency Virus Rev and Herpes Simplex Virus US11. *PLoS One,* 10**,** e0143634.

NOZAWA, Y., VAN BELZEN, N., VAN DER MADE, A. C., DINJENS, W. N. & BOSMAN, F. T. 1996. Expression of nucleophosmin/B23 in normal and neoplastic colorectal mucosa. *J Pathol,* 178**,** 48-52.

OKUWAKI, M., MATSUMOTO, K., TSUJIMOTO, M. & NAGATA, K. 2001. Function of nucleophosmin/B23, a nucleolar acidic protein, as a histone chaperone. *FEBS Lett,* 506**,** 272-6.

OKUWAKI, M., SUMI, A., HISAOKA, M., SAOTOME-NAKAMURA, A., AKASHI, S., NISHIMURA, Y. & NAGATA, K. 2012. Function of homo- and hetero-oligomers of human nucleoplasmin/nucleophosmin family proteins NPM1, NPM2 and NPM3 during sperm chromatin remodeling. *Nucleic Acids Res,* 40**,** 4861-78.

OKUWAKI, M., TSUJIMOTO, M. & NAGATA, K. 2002. The RNA binding activity of a ribosome biogenesis factor, nucleophosmin/B23, is modulated by phosphorylation with a cell cycle-dependent kinase and by association with its subtype. *Mol Biol Cell,* 13**,** 2016-30.

OLSON, M. O., ORRICK, L. R., JONES, C. & BUSCH, H. 1974. Phosphorylation of acid-soluble nucleolar proteins of Novikoff hepatoma ascites cells in vivo. *J Biol Chem,* 249**,** 2823-7.

ORRICK, L. R., OLSON, M. O. & BUSCH, H. 1973. Comparison of nucleolar proteins of normal rat liver and Novikoff hepatoma ascites cells by two-dimensional polyacrylamide gel electrophoresis. *Proc Natl Acad Sci U S A,* 70**,** 1316-20.

OTAKE, Y., SENGUPTA, T. K., BANDYOPADHYAY, S., SPICER, E. K. & FERNANDES, D. J. 2005. Retinoid-induced apoptosis in HL-60 cells is associated with nucleolin down-regulation and destabilization of Bcl-2 mRNA. *Mol Pharmacol,* 67**,** 319-26.

OTAKE, Y., SOUNDARARAJAN, S., SENGUPTA, T. K., KIO, E. A., SMITH, J. C., PINEDA-ROMAN, M., STUART, R. K., SPICER, E. K. & FERNANDES, D. J. 2007. Overexpression of nucleolin in chronic lymphocytic leukemia cells induces stabilization of bcl2 mRNA. *Blood,* 109**,** 3069-75.

PALMIERI, D., RICHMOND, T., PIOVAN, C., SHEETZ, T., ZANESI, N., TROISE, F., JAMES, C., WERNICKE, D., NYEI, F., GORDON, T. J., CONSIGLIO, J., SALVATORE, F., COPPOLA, V., PICHIORRI, F., DE LORENZO, C. & CROCE, C. M. 2015. Human anti-nucleolin recombinant immunoagent for cancer therapy. *Proc Natl Acad Sci U S A,* 112**,** 9418-23.

PELLAR, G. J. & DIMARIO, P. J. 2003. Deletion and site-specific mutagenesis of nucleolin's carboxy GAR domain. *Chromosoma,* 111**,** 461-9.

PIANTA, A., PUPPIN, C., FRANZONI, A., FABBRO, D., DI LORETO, C., BULOTTA, S., DEGANUTO, M., PARON, I., TELL, G., PUXEDDU, E., FILETTI, S., RUSSO, D. & DAMANTE, G. 2010. Nucleophosmin is overexpressed in thyroid tumors. *Biochem Biophys Res Commun,* 397**,** 499-504.

PRINOS, P., LACOSTE, M. C., WONG, J., BONNEAU, A. M. & GEORGES, E. 2011. Mutation of cysteine 21 inhibits nucleophosmin/B23 oligomerization and chaperone activity. *Int J Biochem Mol Biol,* 2**,** 24-30.

QI, W., SHAKALYA, K., STEJSKAL, A., GOLDMAN, A., BEECK, S., COOKE, L. & MAHADEVAN, D. 2008. NSC348884, a nucleophosmin inhibitor disrupts oligomer formation and induces apoptosis in human cancer cells. *Oncogene,* 27**,** 4210-20.

QIN, F. X., SHAO, H. Y., CHEN, X. C., TAN, S., ZHANG, H. J., MIAO, Z. Y., WANG, L., HUI, C. & ZHANG, L. 2011. Knockdown of NPM1 by RNA interference inhibits cells proliferation and induces apoptosis in leukemic cell line. *Int J Med Sci,* 8**,** 287-94.

SAID, E. A., KRUST, B., NISOLE, S., SVAB, J., BRIAND, J. P. & HOVANESSIAN, A. G. 2002. The anti-HIV cytokine midkine binds the cell surface-expressed nucleolin as a low affinity receptor. *J Biol Chem,* 277**,** 37492-502.

SCHMIDT-ZACHMANN, M. S. & NIGG, E. A. 1993. Protein localization to the nucleolus: a search for targeting domains in nucleolin. *J Cell Sci,* 105 (Pt 3)**,** 799-806.

SCHWAB, M. S. & DREYER, C. 1997. Protein phosphorylation sites regulate the function of the bipartite NLS of nucleolin. *Eur J Cell Biol,* 73**,** 287-97.

SCHWARZE, S. R., HO, A., VOCERO-AKBANI, A. & DOWDY, S. F. 1999. In vivo protein transduction: delivery of a biologically active protein into the mouse. *Science,* 285**,** 1569-72.

SERIN, G., JOSEPH, G., GHISOLFI, L., BAUZAN, M., ERARD, M., AMALRIC, F. & BOUVET, P. 1997. Two RNA-binding domains determine the RNA-binding specificity of nucleolin. *J Biol Chem,* 272**,** 13109-16.

SIRRI, V., ROUSSEL, P., TRERE, D., DERENZINI, M. & HERNANDEZ-VERDUN, D. 1995. Amount variability of total and individual Ag-NOR proteins in cells stimulated to proliferate. *J Histochem Cytochem,* 43**,** 887-93.

SOUNDARARAJAN, S., WANG, L., SRIDHARAN, V., CHEN, W., COURTENAY-LUCK, N., JONES, D., SPICER, E. K. & FERNANDES, D. J. 2009. Plasma membrane nucleolin is a receptor for the anticancer aptamer AS1411 in MV4-11 leukemia cells. *Mol Pharmacol,* 76**,** 984-91.

SPECTOR, D. L., OCHS, R. L. & BUSCH, H. 1984. Silver staining, immunofluorescence, and immunoelectron microscopic localization of nucleolar phosphoproteins B23 and C23. *Chromosoma,* 90**,** 139-48.

STORCK, S., THIRY, M. & BOUVET, P. 2009. Conditional knockout of nucleolin in DT40 cells reveals the functional redundancy of its RNA-binding domains. *Biol Cell,* 101**,** 153-67.

SWAMINATHAN, V., KISHORE, A. H., FEBITHA, K. K. & KUNDU, T. K. 2005. Human histone chaperone nucleophosmin enhances acetylation-dependent chromatin transcription. *Mol Cell Biol,* 25**,** 7534-45.

TAHA, M. S., NOURI, K., MILROY, L. G., MOLL, J. M., HERRMANN, C., BRUNSVELD, L., PIEKORZ, R. P. & AHMADIAN, M. R. 2014. Subcellular fractionation and localization studies reveal a direct interaction of the fragile X mental retardation protein (FMRP) with nucleolin. *PLoS One,* 9**,** e91465.

TAKAGI, M., ABSALON, M. J., MCLURE, K. G. & KASTAN, M. B. 2005. Regulation of p53 translation and induction after DNA damage by ribosomal protein L26 and nucleolin. *Cell,* 123**,** 49-63.

TOWBIN, H., STAEHELIN, T. & GORDON, J. 1979. Electrophoretic transfer of proteins from polyacrylamide gels to nitrocellulose sheets: procedure and some applications. *Proc Natl Acad Sci U S A,* 76**,** 4350-4.

TSUI, K. H., CHENG, A. J., CHANG, P., PAN, T. L. & YUNG, B. Y. 2004. Association of nucleophosmin/B23 mRNA expression with clinical outcome in patients with bladder carcinoma. *Urology,* 64**,** 839-44.

UGRINOVA, I., MONIER, K., IVALDI, C., THIRY, M., STORCK, S., MONGELARD, F. & BOUVET, P. 2007. Inactivation of nucleolin leads to nucleolar disruption, cell cycle arrest and defects in centrosome duplication. *BMC Mol Biol,* 8**,** 66.

VUZMAN, D. & LEVY, Y. 2012. Intrinsically disordered regions as affinity tuners in protein-DNA interactions. *Mol Biosyst,* 8**,** 47-57.

WANG, D., BAUMANN, A., SZEBENI, A. & OLSON, M. O. 1994. The nucleic acid binding activity of nucleolar protein B23.1 resides in its carboxyl-terminal end. *J Biol Chem,* 269**,** 30994-8.

WANG, Q. Q., ZHANG, Z. Y., XIAO, J. Y., YI, C., LI, L. Z., HUANG, Y. & YUN, J. P. 2011. Knockdown of nucleophosmin induces S-phase arrest in HepG2 cells. *Chin J Cancer,* 30**,** 853-60.

WANG, W., BUDHU, A., FORGUES, M. & WANG, X. W. 2005. Temporal and spatial control of nucleophosmin by the Ran-Crm1 complex in centrosome duplication. *Nat Cell Biol,* 7**,** 823-30.

XIAO, S., CAGLAR, E., MALDONADO, P., DAS, D., NADEEM, Z., CHI, A., TRINITE, B., LI, X. & SAXENA, A. 2014. Induced expression of nucleolin phosphorylation-deficient mutant confers dominant-negative effect on cell proliferation. *PLoS One,* 9**,** e109858.

XU, Z., JOSHI, N., AGARWAL, A., DAHIYA, S., BITTNER, P., SMITH, E., TAYLOR, S., PIWNICA-WORMS, D., WEBER, J. & LEONARD, J. R. 2012. Knocking down nucleolin expression in gliomas inhibits tumor growth and induces cell cycle arrest. *J Neurooncol,* 108**,** 59-67.

YANG, C., MAIGUEL, D. A. & CARRIER, F. 2002. Identification of nucleolin and nucleophosmin as genotoxic stress-responsive RNA-binding proteins. *Nucleic Acids Res,* 30**,** 2251-60.

YUN, J. P., CHEW, E. C., LIEW, C. T., CHAN, J. Y., JIN, M. L., DING, M. X., FAI, Y. H., LI, H. K., LIANG, X. M. & WU, Q. L. 2003. Nucleophosmin/B23 is a proliferate shuttle protein associated with nuclear matrix. *J Cell Biochem,* 90**,** 1140-8.

YUN, J. P., MIAO, J., CHEN, G. G., TIAN, Q. H., ZHANG, C. Q., XIANG, J., FU, J. & LAI, P. B. 2007. Increased expression of nucleophosmin/B23 in hepatocellular carcinoma and correlation with clinicopathological parameters. *Br J Cancer,* 96**,** 477-84.

YUNG, B. Y. & CHAN, P. K. 1987. Identification and characterization of a hexameric form of nucleolar phosphoprotein B23. *Biochim Biophys Acta,* 925**,** 74-82.

ZATSEPINA, O. V., TODOROV, I. T., PHILIPOVA, R. N., KRACHMAROV, C. P., TRENDELENBURG, M. F. & JORDAN, E. G. 1997. Cell cycle-dependent translocations of a major nucleolar phosphoprotein, B23, and some characteristics of its variants. *Eur J Cell Biol,* 73**,** 58-70.

ZELLER, K. I., HAGGERTY, T. J., BARRETT, J. F., GUO, Q., WONSEY, D. R. & DANG, C. V. 2001. Characterization of nucleophosmin (B23) as a Myc target by scanning chromatin immunoprecipitation. *J Biol Chem,* 276**,** 48285-91.

ZHOU, Y., DU, W., KORETSKY, T., BAGBY, G. C. & PANG, Q. 2008. TAT-mediated intracellular delivery of NPM-derived peptide induces apoptosis in leukemic cells and suppresses leukemogenesis in mice. *Blood,* 112**,** 2474-83.

9 Appendix

MTT HeLa cells	Npmfl	NpmHBD-RNABD	pcDNA3.1flag	mock
	24841	10853	16557	30034
	20713	10136	14567	27323
	21136	9326	16027	27428

Data for Figure 12: MTT assay of nucleophosmin variants in HeLa cells.

MTT Cos-7 cells	Npmfl	NpmHBD-RNABD	pcDNA3.1flag	mock
	13852	9089	10790	19638
	14532	8498	10896	19047
	13417	10021	10786	18896

Data for Figure 12: MTT assay of nucleophosmin variants in Cos-7 cells.

MTT HeLa cells	NclRRM14GAR	NclRRM12	NclRRM34	NclRRM4GAR	NclGAR	pcDNA3.1flag	mock
	9311	10490	10091	10159	10122	16557	30034
	9503	10080	9830	8980	9833	14567	27323
	8373	9758	7712	9775	10037	16027	27428

Data for Figure 13: MTT assay of nucleolin C-terminal variants in HeLa cells.

MTT Cos-7 cells	NclRRM14GAR	NclRRM12	NclRRM34	NclRRM4GAR	NclGAR	pcDNA3.1flag	mock
	8750	10353	10745	8954	9161	10790	19638
	8992	10719	11169	9628	9285	10896	19047
	9045	9933	11435	9196	8191	10786	18896

Data for Figure 13: MTT assay of nucleolin C-terminal variants in Cos-7 cells.

MTT HeLa cells	NclRRM14GAR	NclRRM4GAR	NclGAR	pcDNA3.1flag	mock
	9311	10159	10122	16557	30034
	9503	8980	9833	14567	27323
	8373	9775	10037	16027	27428

Data for Figure 14: MTT assay of nucleolin variants containing GAR in HeLa cells.

MTT Cos-7 cells	NclRRM14GAR	NclRRM4GAR	NclGAR	pcDNA3.1flag	mock
	8750	8954	9161	10790	19638
	8992	9628	9285	10896	19047
	9045	9196	8191	10786	18896

Data for Figure 14: MTT assay of nucleolin variants containing GAR in Cos-7 cells.

FACS HeLa cells	Npmfl	NpmHBd-RNABd	pcDNA3.1flag	mock
	15.62	33.22	18.32	2.86
	14.55	17.35	26.99	3.36
	6.56	14.76	17.74	2.83
	7.53	21.75	15.63	2.43
	4.70	22.66	7.35	2.20

Data for Figure 15: FACS analysis of nucleophosmin variants in HeLa cells (SubG1 cells in %).

FACS Cos-7 cells	Npmfl	NpmHBD-RNABD	pcDNA3.1flag	mock
	1.32	15.68	3.64	3.72
	1.57	6.22	3.95	1.71
	1.49	14.79	2.44	1.52
	1.93	10.14	3.82	1.05

Data for Figure 15: FACS analysis of nucleophosmin variants in Cos-7 cells (SubG1 cells in %).

FACS Cos-7 cells	NclRRM14GAR	NclRRM12	NclRRM34	NclRRM4GAR	NclGAR	pcDNA3.1flag	mock
	8.52	7.91	4.90	4.93	10.19	3.64	3.72
	4.59	4.33	12.54	7.64	8.81	3.95	1.71
	6.51	4.42	9.70	14.25	12.04	2.44	1.52
	2.96	11.29	9.37	11.10	9.50	3.82	1.05

Data for Figure 16: FACS analysis of nucleolin C-terminal variants in Cos-7 cells (SubG1 cells in %).

FACS HeLa cells	NclRRM14GAR	NclRRM12	NclRRM34	NclRRM4GAR	NclGAR	pcDNA3.1flag	mock
	23.82	20.72	22.50	26.66	26.19	18.32	2.86
	15.84	3.33	29.99	44.47	28.00	26.99	3.36
	16.46	4.09	31.67	24.48	17.37	17.74	2.83
	23.04	24.84	36.35	31.25	27.95	15.63	2.43
	11.89	20.78	19.55	22.85	22.63	7.35	2.20

Data for Figure 16: FACS analysis of nucleolin C-terminal variants in HeLa cells (SubG1 cells in %).

FACS HeLa cells	NclRRM14GAR	NclRRM4GAR	NclGAR	pcDNA3.1flag	mock
	23.82	26.66	26.19	18.32	2.86
	15.84	44.47	28.00	26.99	3.36
	16.46	24.48	17.37	17.74	2.83
	23.04	31.25	27.95	15.63	2.43
	11.89	22.85	22.63	7.35	2.20

Data for Figure 17: FACS analysis of nucleolin variants containing GAR in HeLa cells (SubG1 cells in %).

FACS Cos-7 cells	NclRRM14GAR	NclRRM4GAR	NclGAR	pcDNA3.1flag	mock
	8.52	4.93	10.19	3.64	3.72
	4.59	7.64	8.81	3.95	1.71
	6.51	14.25	12.04	2.44	1.52
	2.96	11.10	9.50	3.82	1.05

Data for Figure 17: FACS analysis of nucleolin variants containing GAR in Cos-7 cells (SubG1 cells in %).

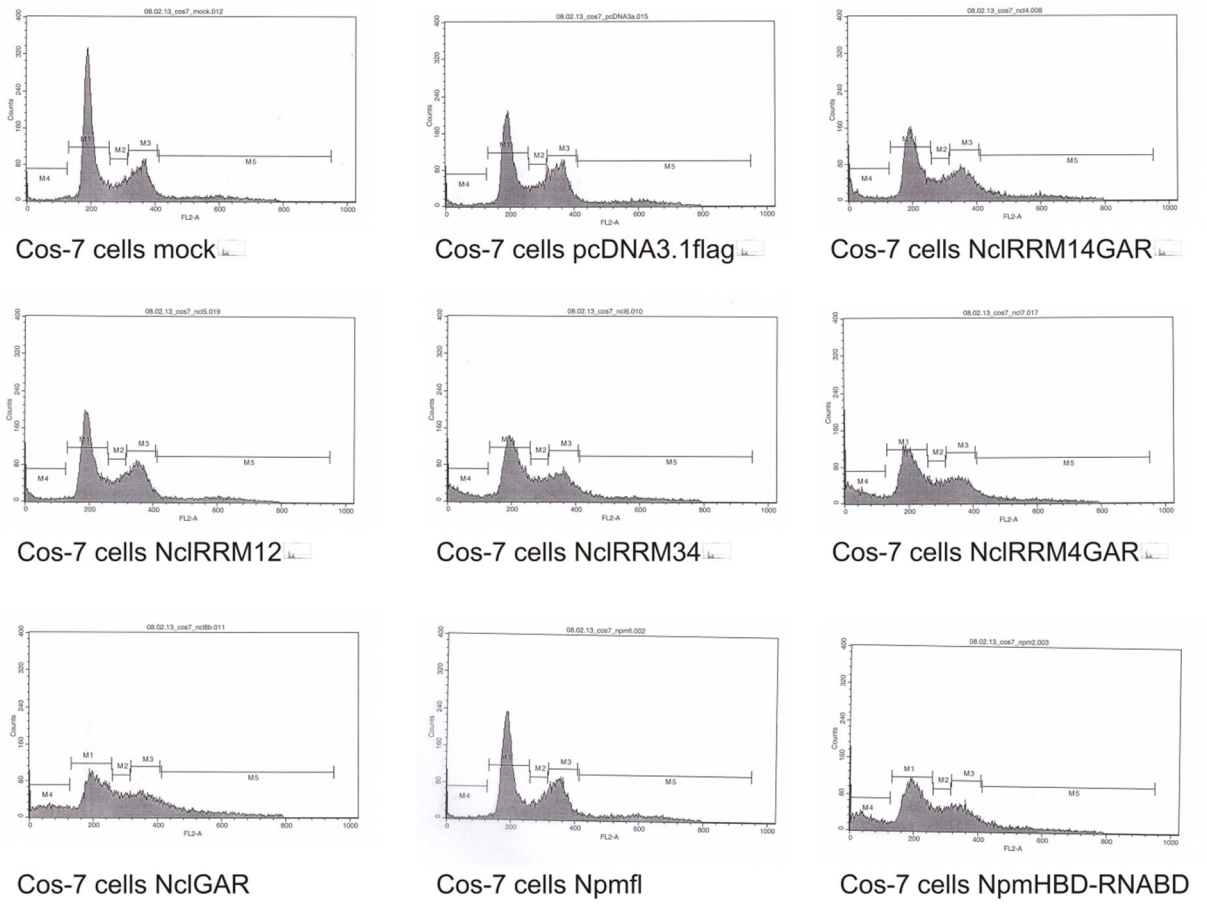

Example for original FACS Data in Cos-7 cells. The amount of SubG1 cells is shown on the very left peak of each figure. The figures belong to the percentages on page 71 marked in red (amount of SubG1 cells in percentages, experiment 3).

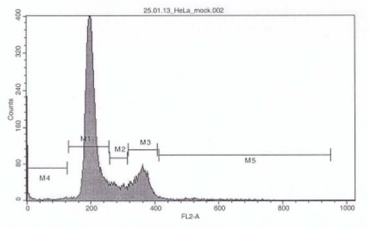
HeLa cells mock

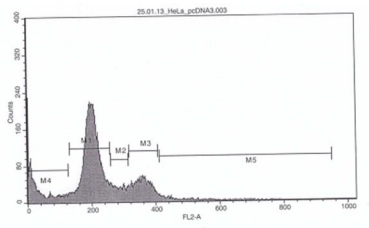
HeLa cells pcDNA3.1flag

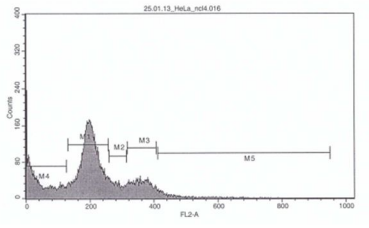
HeLa cells NclRRM14GAR

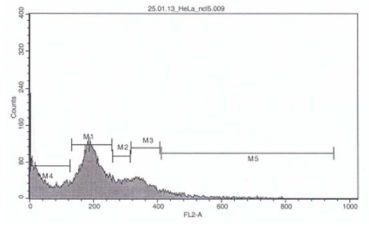
HeLa cells NclRRM12

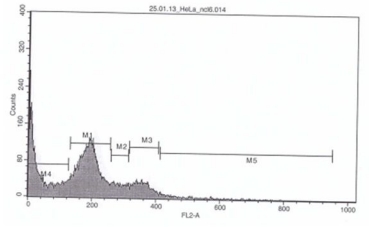
HeLa cells NclRRM34

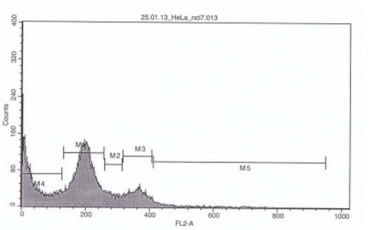
HeLa cells NclRRM4GAR

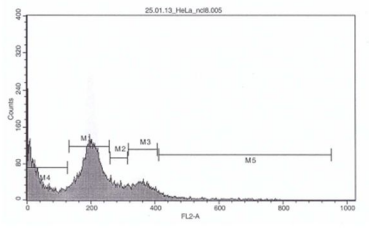
HeLa cells NclGAR

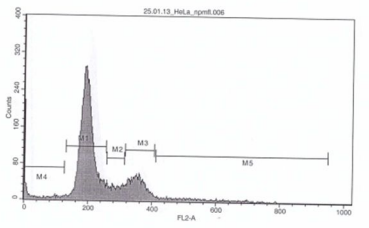
HeLa cells Npmfl

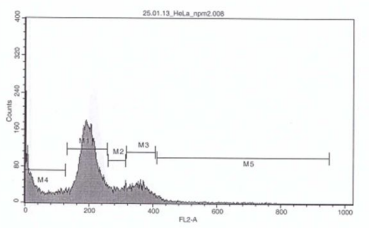
HeLa cells NpmHBD-RNABD

Example for original FACS Data in HeLa cells. The amount of SubG1 cells is shown on the very left peak of each figure. The figures belong to the percentages on page 71 marked in red (amount of SubG1 cells in percentages, experiment 4).

Caspase 3 Cos-7 cells	Npmfl	NpmHBD-RNABD	NclRRM14GAR	NclRRM12	NclRRM34	NclRRM4GAR	NclGAR	pcDNA3.1flag	mock
	1576	3484	3557	3927	3170	4305	3530	3417	1527
	1766	3667	3599	4687	2238	1414	1670	3161	1239
	3061	4332	5100	2881	3935	1712	1240	3698	1109

Data for Figure 18: Caspase 3 assay in Cos-7 cells

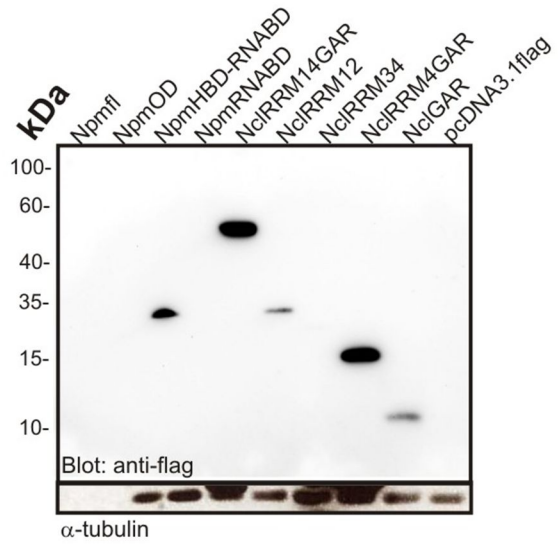

Blot with expression of NclGAR domain for Figure 9

	Npmfl	NpmOD	NpmHB-RNABD	NpmRNABD	NclRRM 14GAR	NclRRM 12	NclRRM 34	NclRRM 4GAR	NclGAR
Experiment1									
Count a	47 %	37 %	50 %		43 %	55 %	39 %	48 %	64 %
Count b	56 %	33 %	64 %		52 %	46 %	26 %	56 %	54 %
Count c	69 %	44 %	72 %		25 %	29 %	35 %	50 %	47 %
Experiment2									
Count a	62 %				52 %	34 %	27 %	47 %	23 %
Count b	35 %				54 %	48 %	35 %	52 %	20 %
Count c	26 %				42 %	32 %	39 %	41 %	29 %
Total efficiency	49.1 %				44.5 %	40.5 %	33.0 %	48.5 %	39.5 %

Table 1: Transfection efficiency of Ncl and Npm variants in HeLa cells (48 h post transfection).
Expression of the nucleolin and nucleophosmin variants in HeLa cells was calculated in percentages, which means the presence of flag-tagged proteins visualized by an anti-flag antibody was set in relation to non-transfected cells visualized by DAPI. The last column presents the total efficiency of the two different experiments with three countings at a 20-fold magnification, respectively. It was not possible to detect any anti-flag signal for the NpmRNABD variant. The second experiment for the NpmOD and NpmHB-RNABD variants did not show sufficient fluorescence signals.

10 Acknowledgements

My first and special thanks go to my supervisor Prof. Dr. Reza Ahmadian for the provision of the topic of this thesis, the assessment, comments and suggestions without which this work would not have been possible. He gave me the opportunity to be a part of his research group and I am highly grateful for his advice which was always helpful. I honour him for his constant support and his striking group leading abilities. I am indeed very thankful for his encouragement for finalizing the last draft of this thesis. Furthermore, I would like to thank his whole research group for their support and unforgettable moments in the laboratory.

I would like to thank Dr. Jens Moll for all his valuable input, support in the laboratory and the proofreading of this thesis. I am extremely thankful to Dr. Kazem Nouri and Dr. Saeideh Nakhaei-Rad for their assistance and technical advice. I would also like to gratefully acknowledge helpful suggestions from Dr. Roland Piekorz.

Lastly, I would like to thank the whole Institute for Biochemistry and Molecular Biology II of the Heinrich-Heine-University in Düsseldorf for their great support over the last years.

I gratefully acknowledge the financial support of the research commission of the Heinrich-Heine-University Düsseldorf (project 9772523).

11 Statutory Declaration

Ich versichere an Eides statt, dass die Dissertation selbständig und ohne unzulässige fremde Hilfe erstellt und die hier vorgelegte Dissertation nicht von einer anderen Medizinischen Fakultät abgelehnt worden ist.

Datum, Vor- und Nachname

Unterschrift